SOIL CARBON ASSESSMENT: CONFRONTING CLIMATE CHANGE ON THE FARM

A Thesis

Presented to the Faculty of the Graduate School

of Cornell University

In Partial Fulfillment of the Requirements for the Degree of

Master of Science

by

Jeffrey Prescott Beem-Miller

August 2017

ABSTRACT

Reductions in greenhouse gas emissions must be complimented with increases in negative emissions in order to stabilize atmospheric carbon dioxide concentrations and prevent catastrophic changes in climate. Soil carbon sequestration on arable lands is a negative emissions technology with high climate change mitigation potential that also confers agronomic co-benefits, but variability of soil organic carbon (SOC) stocks remains both a statistical and financial challenge for verifying SOC sequestration goals. This work is in two parts: 1) improving sampling methods for SOC assessment on rocky soils, and 2) reducing sampling requirements for mapping and modeling field-scale subsoil, topsoil and whole profile SOC stocks via remote and proximal sensing. Part 1 shows that hammer corers bias SOC stock estimates, while rotary corers are more accurate on rocky soils; and that SOC stocks should be calculated and reported on a mass-basis for improved accuracy and precision. Part 2 shows that proximal sensing with tractor-mounted visual/near-infrared spectroscopy (VNIR-p) is an effective approach for stratification and mapping of topsoil (0-0.30 m) and profile (0-0.75 m) SOC stocks with a reduced sample number (n=12 cores); however, due to the greater spatial covariance of SOC stocks over shorter distances in subsoil compared to topsoil, VNIR-p does not adequately capture the distribution of SOC stocks in subsoil.

BIOGRAPHICAL SKETCH

Jeffrey Prescott Beem-Miller was born and raised in the glacially carved hills and hanging valleys of the Finger Lakes Region in Upstate New York. Brought up among the beauty of the fields and forests, and encouraged to spend as much time as possible outdoors, he knew from the age of four that he would pursue a career in science. He attended Oberlin College for his Bachelor's degree, which he earned in the fields of Biology, and Environmental Studies. Interest in education and a desire to explore the mountains sent him west to Colorado, where he taught at a nature center, and then on to Nevada, where he worked as a field botanist with the United States Bureau of Land Management. Returning to Ithaca to be with his family, he also returned to academia, and began working with Professors Fahey and Yavitt, studying forest ecology with an emphasis on soil carbon in the Department of Natural Resources at Cornell University. A desire to gain experience in agriculture, with an eye towards conservation and sustainable development, brought him into a laboratory manager position with Professor Wolfe in the Cornell Department of Horticulture. Working in the Wolfe Lab on a collaborative project seeking to develop new tools for carbon, nitrogen, and greenhouse gas accounting and management in corn cropping systems, Jeffrey decided to expand on this work with a Master's degree. Starting in September 2017, Jeffrey will be matriculating in a PhD program at the Max Planck Institute for Biogeochemistry in Jena, Germany, where he will be studying the global carbon cycle with Drs. Susan Trumbore, Carlos Sierra, and Marion Schrumpf.

Dedicated to my Mother, whose love will motivate me always; and my Father, who has never let me down

ACKNOWLEDGMENTS

My fiancée Dora, whose love and encouragement knows no bounds; my family; my advisor Dave Wolfe, and the Wolfe Lab crew, Sonam Sherpa, Jonathan Comstock, et al.; Johannes Lehmann; scientific mentors and teachers from elementary school through Cornell University; colleagues in the Horticulture Department; and the United States Department of Agriculture grant no. 2011-67003-30205.

TABLE OF CONTENTS

LIST OF FIGURES

LIST OF TABLES

Chapter 1: Sampling for Soil Carbon Stock Assessment in Rocky Agricultural Soils

ABSTRACT

Coring methods commonly employed in soil organic C (SOC) stock assessment may not accurately capture soil rock fragment (RF) content or soil bulk density (BD) in rocky agricultural soils, potentially biasing SOC stock estimates. Quantitative pits are considered less biased than coring methods, but are invasive and often cost-prohibitive. We compared fixed-depth and mass-based estimates of SOC stocks (0.3-m depth) for hammer, hydraulic push, and rotary coring methods relative to quantitative pits at four agricultural sites ranging in RF content from <0.01 to 0.24 m^3 m^{-3}. Sampling costs were also compared. Coring methods significantly underestimated RF content at all rocky sites, but significant differences ($p < 0.05$) in SOC stocks between pits and corers were only found with the hammer method using the fixed-depth approach at the <0.01 m^3 m^{-3} RF site [pit 5.80 kg C m^{-2}, hammer 4.74 g C m^{-2}] and at the 0.14 m^3 m^{-3} RF site [pit 8.81 kg C m^{-2}, hammer 6.71 kg C m^{-2}]. The hammer corer also underestimated BD at all sites, as did the hydraulic push corer at the 0.21 m^3 m^{-3} RF site. No significant differences in mass-based SOC stock estimates were observed between pits and corers. Our results indicate that: 1) calculating SOC stocks on a mass basis can overcome biases in RF and BD estimates introduced by sampling equipment, and 2) a quantitative pit is the optimal sampling method for establishing reference soil masses, followed by rotary, then hydraulic push corers.

1.1. INTRODUCTION

Given the importance of soil as the largest terrestrial C pool, substantial effort has been made to quantify and monitor SOC stocks in recent decades. Agricultural systems are of particular interest in this context, due to the potential for management practices to influence sequestration of atmospheric C, and the positive impact of SOC as soil organic matter on soil fertility, water holding capacity, and drainage (West and Post, 2002; Lal, 2009; CAST 2011). Maintaining or increasing the soil C pool in agricultural systems is a promising tool for mitigation of global climate change, and is considered to be a relatively inexpensive option for meeting greenhouse gas emission reduction targets (Conant et al., 2011; Wolfe, 2013). However, RF, defined as mineral material greater than 2 mm in diameter, can present a challenge for obtaining representative soil samples for SOC stock assessment and contribute substantial error to SOC stock estimates (Gifford and Roderick, 2003; Harrison et al., 2003; Goidts et al., 2009; Bornemann et al., 2011; Schrumpf et al., 2011; Hedley et al., 2012; Hoffmann et al., 2014). In a study looking at sources of error in an assessment of SOC stocks in Southern Belgium, Goidts et al. (2009) found RF to be the main source of variability in SOC stocks for rocky arable soils (defined as > 0.09 m^3 m^{-3} RF). Hedley et al. (2012) found greater uncertainty in SOC stock estimates in rocky soils (defined as > 0.05 m^3 m^{-3} RF) than non-rocky soils, despite using a labor-intensive pit method for sample collection to improve accuracy of RF and BD measurements at the rocky sites.

Improving our ability to measure SOC stocks in rocky soils is an issue of global importance as these soils are widespread. For example, more than 60% of land area in the Mediterranean region is characterized as rocky (Poesen and Lavee, 1994), 33% of soils in the contiguous 48 states of the US have >35% RF (Throop et al., 2012, Figure 3), and 16% of US

arable land is rocky (Miller and Guthrie, 1984). Additionally, the proportion of arable soils with high RF content is expected to increase due to erosion and cultivation of marginal lands (Bornemann et al., 2011). While several studies have investigated different methods of sampling SOC pools in rocky forest systems (e.g., Vadeboncoeur et al., 2012; Mehler et al., 2014; Xu et al., 2016), relatively few have addressed the issue in agricultural systems. Rytter (2012) reported that neglecting even moderate volumes of stone and gravel (~0.08 m^3 m^{-3}) can lead to overestimation of C stocks in arable sites.

Measuring and monitoring SOC stocks requires quantification of OC and BD. The proportion of RF is also important, as RF content not only determines the volume of soil available for C storage, but can affect both OC and BD (Xu et al., 2016). Fine-earth BD has been shown to be inversely correlated with RF content, although the exact relationship depends on the texture of the soil and both the size and shape of the RF (Stewart et al., 1970; Poesen and Lavee, 1994). The relationship between RF and OC can be either negative or positive: Bornemann et al. (2011) found evidence of an increase in OC in the rockier areas of an agricultural field, but others have found a negative relationship between OC and RF (Ferrara et al., 2012).

Soil organic C stocks are commonly expressed as a unit mass of C per unit area at a defined soil depth [Eq. 1]:

$$SOC_{stock}\ (kg\ m^{-2}) = OC\ \cdot BD_{FE} \cdot depth\ \cdot (1 - RF) \qquad [1]$$

Where OC (kg kg^{-1}) is the organic C content of the fine-earth <2 mm, BD_{FE} is the fine-earth bulk density (kg m^{-3}), depth is the depth of sampling as measured from the soil surface (m), and RF is the volumetric proportion of rock fragments >2 mm (m^3 m^{-3}).

Organic C content tends to be more spatially variable than BD, requiring more samples (Adhikari et al., 2014), but BD requires a larger sample volume than OC for accurate measurement (Vincent and Chadwick, 1994). The RF content of arable soils tends to be both highly spatially variable (Schrumpf et al., 2011) and require large sample volume to measure accurately (Buchter et al., 1994; Vincent and Chadwick, 1994). Spatial variability and the precision and accuracy with which OC, BD, RF, and depth are measured necessitate compromise between the cost of collecting and analyzing samples, and obtaining a sufficient number of samples to meet an acceptable level of error (Mäkipää et al., 2008).

Soil sampling methods play a key role in determining the cost of sampling and can have a potentially significant effect on estimates of RF content, BD, and soil mass when sampling in rocky soils (Kulmatiski et al., 2003; Rau et al., 2011; Vadeboncoeur et al., 2012). Common soil sampling methods can be classified in three general categories: excavation, clod, and coring methods (Soil Survey Laboratory Staff, 2004). Excavation methods, such as the quantitative soil pit, are assumed to be the most accurate and least biased of the three when it comes to measuring soil mass and RF, because these properties can be measured directly on a large volume of sample (Harrison et al., 2003; Johnson et al., 2010). Soil mass and volume can also be directly measured with clod methods, but the method is not appropriate in soils with abundant RF, as clods do not typically represent the particle distribution of RF (Kimble et al., 2001; Harrison et al., 2003; Soil Survey Laboratory Staff, 2004).

Different driving mechanisms employed by coring methods (e.g., pushing, hammering, or rotating) can compact or loosen the soil during sample collection, introducing bias into the measurement of soil volume (Page-Dumroese et al., 1999; Gifford and Roderick, 2003). For example, on a forest soil with an RF content of 0.31 m^3 m^{-3} and BD of 940 kg m^{-3} (as estimated

by 0.5-m^2 quantitative pits to a depth of 0.15 m), Kulmatiski et al. (2003) found that hammer coring significantly (p = 0.0001) underestimated RF content by 87% and BD by 19%. Soil corer dimensions are a further source of bias in RF and BD estimates on rocky soils. Rocks larger than the diameter of the core prevent coring, while rocks smaller than the core diameter can still restrict core insertion, in either case requiring coring at another location, and thus underestimating RF (Throop et al., 2012). In spite of these limitations, soil corers have the advantage of requiring less site disturbance than excavation methods, often an important consideration when working in agricultural systems or in a research plot, and usually cost less on a per sample basis than the other methods. Kulmatiski et al. (2003) reported that excavating a single pit sample required 3.5 person-hours whereas approximately 12 hammer cores could be collected in the same amount of time. However, when multiple attempts are needed to extract a core in rocky sites, this cost advantage decreases. Given the potential for underestimating RF and introducing bias in soil mass estimates when using coring methods, the predominance of this approach in SOC stock assessment studies could be misrepresenting SOC stocks in sites with high RF (Throop et al., 2012), or could be contributing to unrecognized errors in monitoring schemes in which different types of corers are employed.

A further source of error in estimating SOC stocks over space and time can arise from calculating and reporting SOC stocks to a fixed depth (Eq. 1). When comparing the effect of management such as tillage, or other practices that influence both BD and OC, estimates of SOC stocks based on the measurement of depth from the soil surface can lead to errors (Wuest, 2009; Schrumpf et al., 2011). One solution to this issue is to report SOC stocks on a mass basis, in other words reporting the content of OC in a pre-determined reference mass of soil, rather than to a specific depth (Ellert et al., 2001). In a seminal study, Ellert and Bettany (1995) found

substantial differences between estimates of SOC stocks when they used a mass-based approach to reevaluate a number of studies where changes in SOC stocks as a response to management had been initially evaluated on a fixed-depth basis. Similar to the comparison of SOC stocks for soils under different management, estimates of SOC stocks among soils with different RF content can also vary depending on whether fixed-depth or mass-based approaches are used. With the fixed-depth approach, RF are treated as voids, whereas with mass-based approaches, the mass or volume of RF is replaced by soil from deeper in the profile when calculating SOC stocks to reach the established reference soil mass (Ellert and Bettany, 1995; Lee et al., 2009; Schrumpf et al., 2011). The mass-based approach is increasingly recommended for monitoring and measuring SOC stocks (Gifford and Roderick, 2003; IPCC 2006; Vandenbygaart, 2006; Lee et al., 2009 Minasny et al., 2013; Wendt and Hauser, 2013; Rovira et al., 2015). However, to our knowledge the effect of sampling equipment bias on SOC stocks calculated on a mass-basis has not been evaluated.

Identifying and quantifying the biases introduced by sampling equipment, as well as the relationship between sampling equipment and soil RF content, are critical for improving accuracy and reducing uncertainty in SOC stock assessments. Moreover, the application of the mass-based approach when estimating SOC stocks on rocky soils is not well-studied, nor are the associated costs for sample collection and processing with different sampling equipment well-quantified in the literature. The objectives of this study were to:

1. Evaluate the precision and accuracy of SOC stock estimates and the associated parameters (BD, RF, OC, and depth) for three coring methods, hydraulic push, hammer, and rotary, by comparison to the quantitative pit method at four sites ranging in RF content from <0.01 to 0.24 m^3 m^{-3}.

2. Compare fixed-depth and mass-based approaches to estimating SOC stocks among sampling methods; and
3. Provide estimates of the cost of sampling, including field, laboratory, and equipment costs, for each sampling method at the sites with the highest (0.24 m^3 m^{-3}) and lowest RF content (<0.01 m^3 m^{-3}).

1.2. MATERIALS AND METHODS

1.2.1. Sampling Sites

Soil samples were collected at four sites located on two farms operated by Cornell University: the Homer Thompson Vegetable Farm (42° 26' 13" N, -76° 14' 7" W) and the Animal Teaching and Research Center (42° 31' 4" N, -76° 19' 56" W). The farms are located approximately 11.2 km apart in the Finger Lakes region of New York State, USA. Mean annual precipitation is 104 cm and the mean annual temperature is 7.3 °C. The sampling sites were selected to represent agricultural soils typical for the region, with a range of RF contents, though not so rocky as to substantially restrict tillage. Sites were labeled according to pit estimated RF content: RF <0.01, RF 0.14, RF 0.21, and RF 0.24 m^3 m^{-3}. Preliminary sampling was conducted to ensure sites included a range of RF content. Soils at sites RF 0.14 (Animal Teaching and Research Center), RF 0.21 (Homer Thompson Vegetable Farm), and RF 0.24 (Homer Thompson Vegetable Farm) were Howard gravelly loams (loamy-skeletal, mixed, active, mesic Glossic Hapludalfs), formed in medium textured glacial outwash deposits. Soils at the RF <0.01 site (Homer Thompson Vegetable Farm) were Eel silt loams (fine-loamy, mixed, super-active, mesic, Fluvaquentic Eutrudepts), formed in alluvium. All sampling sites were cultivated fields with <3% slope. Cropping systems at the <0.01, 0.21, and 0.24 m^3 m^{-3} RF sites consisted of vegetable

Table 1.1 Overview of sampling methods compared in this study.

Sampling Method	Core Diameter	Sample Area	Equipment Cost	Operational Cost	Pros	Cons
	mm	mm^2				
Quantitative Pit	NA	500,000	Low	High	Large sample area; accuracy; minimal bias against rocks	Laborious; large quantity of sample; invasive
Rotary	101.6	81,000	Moderate	Low	Minimal bias against subsurface rocks; portable; spatial coverage	Custom assembly; maximum 10 to 15-cm increments; cannot collect intact cores
Hydraulic Push	38.1	1,100	High	Low	Ease of use (hydraulic); spatial coverage; intact cores	Expensive; requires tractor or truck, soil compaction potential; core compaction potential
Hammer	30.0	700	Moderate	Moderate	Ease of use; spatial coverage; portable; storage (liner)	High rock bias; core compaction/loosening potential; moderately expensive

production with a rye (*Secale ceraeale*) cover crop. Site RF 0.14, at the Animal Teaching and Research Farm, had silage corn (*Zea mays*) in rotation with alfalfa (*Medicago sativa*), and also received substantial manure applications annually (38.5 kL ha^{-1} liquid and 8.3 Mg ha^{-1} solid). Sampling was conducted at the Homer Thompson Vegetable Farm over two weeks in October 2013 and at the Animal Teaching and Research Center over one week in May 2014. The M sampling was conducted after it was determined that an additional site with an intermediate RF content between <0.01 and 0.21 m^3 m^{-3} would strengthen the study.

1.2.2. Sampling Design

At each site, three replicate plots spaced 15 m apart were sampled along a transect parallel to the field edge. No samples were collected closer than 5 m to the field edge. Soil sampling was conducted with the following methods: 1) quantitative soil pit, 2) rotary corer, 3) hydraulic push corer, and 4) hammer corer (Table 1.1). One quantitative pit was excavated at the center of each plot (n = 3 at each site), and three replicate cores were extracted for each coring method at distances of 1, 2, and 3 m from the center of the pit (n = 9 at each site; Figure 1.1).

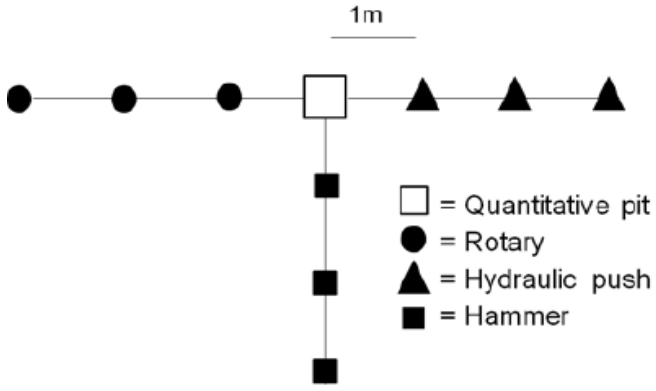

Figure 1.1 Plot layout at the four sites: <0.01, 0.14, 0.21, and 0.24 m^3 m^{-3} rock fragment content. Three plots were sampled per site.

Samples were not collected from the fourth side of the pit in order to provide space for excavation of the pit, while minimizing site disturbance prior to coring. Similarly, coring methods were isolated on separate axes in order to minimize site disturbance and to facilitate operation of the vehicle required for the trailer-mounted hydraulic push sampler. All samples were collected to a depth of 0.30 m, in 0.10-m depth increments, and each 0.10-m increment was analyzed individually.

1.2.3. Quantitative Pits

Quantitative soil pits were excavated according to the method of Vadeboncoeur et al. (2012). Briefly, a rectangular wooden frame with an interior area of 0.5 m^2 was centered over a pin flag placed on the main transect. The pit was moved if the site was highly uneven, i.e., deep furrows or wheel ruts. The frame was secured by driving four 0.5-m-long rebar stakes (9.5-mm o.d.) through holes drilled in the frame and held in place with u-bolts. Aboveground vegetation was minimal, and when present was removed with clippers. Pits were excavated in 0.10-m increments using square-bladed shovels, trowels, and stiff putty scrapers. Depth measurements (pit floor to the bottom of the frame) were taken at 25 equally spaced points and averaged for each increment; a 0.707-m section of 38-mm x 89-mm lumber was used to check length and width of the pit. All material removed from the pit was weighed to the nearest gram and placed through a 12-mm sieve in the field. For the first pit excavated at each site, the >12-mm fraction was weighed, after brushing off adhered soil by hand, and placed in bags for size class distribution analysis in the laboratory. Replicates from preliminary sampling did not show substantial variation in size class distribution, and so for the remaining two pits, the weight of the >12-mm material was recorded and the material was then returned to the field. The <12-mm material for each 0.10-m depth increment was collected on a tarp and homogenized with a

shovel. Approximately 0.5–0.8 kg per depth increment of homogenized material was subsampled and brought back to the laboratory in sealed plastic bags. This field sieving and subsampling procedure was adopted from Vadebonceour, et al. (2012) to reduce the amount of sample transported back to the laboratory.

1.2.4. Rotary Corer

We constructed a rotary coring sampling apparatus similar to that described in Rau, et al. (2011) by mounting a diamond-tipped coring bit (101.6 mm i.d.; Lackmond Products, Inc., Marietta, GA) to a motorized powerhead (Briggs and Stratton, Milwaukee, WI). After drilling each 0.10-m depth increment, the coring apparatus was carefully lifted out of the sampling hole to prevent crumbling of the sidewall and set down on a flexible plastic cutting mat. All material was removed from the core, collected on the mat, and then transferred to a sealable plastic sample bag. To prevent lateral movement of the corer, the bit was braced against the operators' feet for the 0–0.10-m increment. Cores were discarded if any lateral movement of the corer or crumbling of the sidewall was observed.

1.2.5. Hydraulic Push Corer

The hydraulic push sampling method used a trailer-mounted hydraulic soil sampler (Giddings Machine Company, Fort Collins, CO) with a 38.1-mm i.d. coring probe attached. Cores were cut into 0.10-m increments in the field and placed in separate sealable plastic bags.

1.2.6. Hammer Corer

The hammer coring method employed an electric hydraulic jack hammer fitted with a hammer cup attachment to drive a 30.0-mm i.d. stainless steel coring probe (JMC Soil Samplers, Newton, IA) etched with 10-cm increment markings. A plastic tube liner was inserted into the probe to facilitate removal of intact cores. After every 0.10 m of coring we inserted a meter stick

into the opening at the top of the probe to measure the height of the soil inside the corer relative to the soil surface in order to obtain a measure of potential compaction for each depth increment. Once the probe reached the 0.30-m mark, it was extracted with a spring-driven, foot-pedal-operated jack.

For all coring methods the surface soil was dampened with water from a spray bottle before coring to minimize crumbling of the sidewall. We also measured the depth of the bore hole for each sampling method after cores were removed to allow us to assess compaction, and to verify that the core did not break during extraction. For the hydraulic push and hammer methods, cores with an extracted length less than 0.24 m (20% of the target depth of 0.30 m) were discarded. While 20% is a substantial difference between target and extracted depth, previous experience sampling soils with up to 0.50 m^3 m^{-3} RF led us to set this minimum requirement as realistic for ensuring the collection of an adequate number of soil cores. If a core ≥0.24 m could not be obtained after eight attempts, or if extracted cores contained gouges >5% by volume (based on a visual inspection), no core was collected at that location. For all methods, soil samples were placed on ice in the field, transported to the lab, and stored at 5 °C until further processing.

1.2.7. Laboratory Analysis

All soil samples were weighed at field moisture; for the pit and rotary coring methods, 0.3 to 0.5 kg of field-moist soil were subsampled using a riffle box sample splitter (Humboldt, Elgin, IL). Soils were sieved (<2-mm) and dried at 35 °C for 48 h in a convection oven. Subsamples of the <2-mm soil were analyzed for total C concentration by dry combustion (LECO CN 2000, St. Joseph, MI). Although no endogenous carbonates were expected with these soils, samples were screened for carbonates with a qualitative effervescence test using dilute

hydrochloric acid (Soil Survey Laboratory Staff, 2004). Moisture content was determined on separate subsamples (~20 g field moist soil) dried at 35 °C for 48 h in a convection oven, weighed, and then weighed again after further drying at 105 °C until no change in weight was detected. Moisture content subsamples were then sieved to 2 mm. Material >2 mm was washed, dried overnight at 105 °C, and weighed. An average particle density of 2650 kg m^{-3} was used for the >2-mm fraction to determine the volume, based on the density of shale, the dominant rock type of the samples (Neeley, 1965; Levine et al., 2012). Rock fragments were then further separated into three size classes, 2–12, 12–38, and >38 mm, and weighed again.

1.2.8. Estimating Bulk Density and Soil Volume

Bulk density can be calculated in various ways. One common approach considers the BD of the fine earth (BD_{FE}):

$$BD_{FE} = \frac{M_{core} - M_{rock}}{V_{core} - V_{rock}} \quad [2]$$

Where M_{core} is the total dry mass of the soil core (kg), M_{rock} is the mass of the RF (kg), V_{core} is the total volume of the core (m^3), and V_{rock} is the volume of the RF fraction (m^3).

However, determining V_{rock} requires using an assumed rock density (for example 2650 kg m^{-3}), or a labor-intensive direct measure of V_{rock}, like water displacement. Throop et al. (2012) suggested a simpler approach to estimating BD in rocky soils, where BD is calculated as the mass of the oven-dried (105 °C) fine earth (<2-mm) fraction over the total volume of the core:

$$BD = \frac{M_{core} - M_{rock}}{V_{core}} \quad [3]$$

This formulation of BD is useful for calculating SOC stock as it obviates calculating RF volume directly.

Intact core methods, such as the hammer and hydraulic push methods in this study, yield an additional measurement of core-length, which can be used to assess whether compaction or loosening of the soil occurred during coring, or whether obstruction from RF may have prevented soil from entering the core. The V_{core} term in Eq. [3] can be calculated using either the length of the extracted core or the depth of the bore hole, generating two different estimates of BD, $BD_{Core\text{-}Length}$ (Eq. [4]) or $BD_{Hole\text{-}Depth}$ (Eq. [5]), respectively.

$$BD_{Core-Length} = \frac{M_{core}-M_{rock}}{V_{core,Core-Length}} \quad [4]$$

$$BD_{Hole-Depth} = \frac{M_{core}-M_{rock}}{V_{core,Hole-Depth}} \quad [5]$$

Where $V_{core,Core\text{-}Length}$ is the length of the extracted core (m) multiplied by the cross-sectional area of the corer (m^2), and $V_{core,Hole\text{-}Depth}$ is the depth of the bore hole (m) multiplied by the cross-sectional area of the corer (m^2). Using the length of the extracted core in the calculation of $BD_{Core\text{-}Length}$ assumes that the discrepancy between the length of the core and the depth of the bore hole is due to exclusion of soil, such as obstruction by RF. Using the depth of the bore hole to calculate BD_{Hole_Depth} assumes that any difference between core length and hole depth is due to compaction or loosening of the soil during coring or extraction. For example, consider a soil core with a mass of 0.22 kg, collected with a 30-mm diameter core. If the length of the extracted core is 0.25 m, and the depth of the bore hole is 0.30 m, $BD_{Core\text{-}Length}$ would be 1245 kg m^{-3} and $BD_{Hole\text{-}Depth}$ would be 1038 kg m^{-3}, a substantial difference.

1.2.9. SOC Stock Calculation

Soil organic C stocks were calculated using both fixed-depth and mass-based methods. Preliminary data analysis showed few significant differences between depth increments in OC content for these tilled plots (data not shown), so all data were cumulatively analyzed for the 0-0.3-m depth profile. Fixed-depth SOC stocks were calculated using both $BD_{Core\text{-}Length}$ (Eq. [6]) and $BD_{Hole\text{-}Depth}$ (Eq. [7]):

$$SOC_{Core-Length} kg\ m^{-2} = BD_{Core-Length} kg\ m^{-3} \cdot depth\ m \cdot OC\ kg\ kg^{-1} \quad [6]$$

$$SOC_{Hole-Depth} kg\ m^{-2} = BD_{Hole-Depth} kg\ m^{-3} \cdot depth\ m \cdot OC\ kg\ kg^{-1} \quad [7]$$

For the mass-based SOC stock estimation approach, we used the procedure of Wendt and Hauser (2013). This approach does not use sampling depth, nor does it require the calculation of BD, but rather relies on the relationship between soil mass and soil C mass in order to interpolate SOC stocks at an established reference mass. First, we calculated areal soil mass for each depth increment (0-0.1, 0.1-0.2, 0.2-0.3 m) as the total dry soil mass (< 2 mm) over area sampled. We then calculated OC mass layers for each depth increment by multiplying areal soil mass by mean OC concentration. We fit a cubic spline function to model the relationship between the raw cumulative areal soil mass (0-0.3 m) and cumulative OC mass (0-0.3 m). Using this relationship, SOC stocks can then be calculated for any desired reference mass of soil, rather than being fixed at a particular depth. We used mean cumulative areal soil mass as estimated by the quantitative pit method for 0.3-m of soil at each site as a reference mass.

1.2.10. Data Analysis

A linear mixed-effect model (JMP Pro software, version 11.0, SAS Institute) was used to compare RF in each size class (2–12, 12–38, >38 mm, and total RF > 2 mm), BD ($BD_{Core\text{-}Length}$,

$BD_{Hole\text{-}Depth}$), OC, and SOC stocks ($SOC_{Core\text{-}Length}$, $SOC_{Hole\text{-}Depth,}$ and $SOC_{Mass\text{-}Based}$). Main effects for the RF, OC, BD, and SOC models were sampling method, site, and the interaction between site and sampling method, with plot as a random blocking factor. Additional fixed effects for the BD and SOC models included calculation method, and all associated interactions. Pairwise comparisons among means within site and calculation method were conducted using the Bonferroni adjustment. Effects were deemed significant at $p < 0.05$ unless otherwise noted. SOC stocks were also assessed on the basis of normalized differences between pit and corer estimates. Differences were normalized by subtracting pit estimates of SOC stocks from corer estimates, and dividing the difference by pit estimates.

Simple linear regression was used to compare estimates of BD from the pit method to corer estimates. For the regression analysis, data from the coring methods were averaged by plot to balance the number of samples between pit and coring methods, since three replicate cores to one pit sample were collected from each plot. Regressions were performed in R (R, 2013).

We used the delta method of error propagation to calculate the error contributed by each factor in the fixed-depth SOC stock equations (Eqs. [6] and [7]) (Goidts et al., 2009; Schrumpf et al., 2011). The delta method uses a linear Taylor series expansion to determine the total random error on SOC stocks (Var_{total}, Eq. [8]) contributed by the variance of BD (*Var BD*), the variance of OC (*Var OC*), and the covariance between BD and OC (*Cov OC-BD*). The proportion of Var_{total} due to the variance and covariance of these factors was calculated as the value of each of the terms in the sum in Equation [8] divided by the sum of the absolute values of each of those terms. This calculation was performed separately for $SOC_{Core\text{-}Length}$ and $SOC_{Hole\text{-}Depth}$ for intact core methods, using $BD_{Hole\text{-}Depth}$ and $BD_{Core\text{-}Length}$, respectively. This approach was not applied to

the mass-based method, however, as the relative contribution of each term to total error is not available from a spline function (Press et al., 2007).

$$Var_{total} = SOC\ stock^2 \times \left(\frac{Var\ OC^2}{OC^2} + \frac{Var\ BD^2}{BD^2} + 2 \times \frac{Cov\ OC{-}BD^2}{BD \cdot OC^2}\right) \quad [8]$$

1.2.11. Cost Estimation

Cost estimates for measuring SOC stocks with each of the four sampling methods were made for the RF 0.24 and RF <0.01 $m^3\ m^{-3}$ sites. We calculated fixed and variable costs separately (Mäkipää et al., 2008; Singh et al., 2013). Total variable cost per sample was calculated as the sum of variable equipment costs, sample collection costs, and sample analysis costs. The only fixed cost considered was the overhead cost of sampling equipment. All cost estimates were based on US dollars in 2013.

Sample collection costs were calculated as the product of the operator-hours per sample and the operator wages. Operator wages were set at US $15. Operator-hours per sample were based on the number of operators required, the time from arrival to departure, and the number of samples collected in that time. The amount of time required for sampling depends on both soil and weather conditions, so we made an effort in this study to ensure weather and soil conditions were similar across sampling events in order to facilitate equal comparison of sampling methods within and across sites.

Sample analysis costs were calculated as the time required per sample in the laboratory to prepare samples for OC analysis, including subsampling, sieving, and moisture content analysis. Time and analytical costs for OC analysis were not compared, as they were the same for all sampling methods. Variable equipment cost included the cost of sample collection bags (for the

hydraulic push, rotary, and pit methods) or tube liners (for the hammer method), multiplied by the number of samples. The cost of all other tools and equipment were considered fixed costs.

1.3. RESULTS & DISCUSSION

1.3.1. Sampling Method and Calculation Approach Effects on Estimates of RF, BD, and OC

Our first objective was to evaluate the precision and accuracy of sampling for BD, RF, and OC using rotary, hydraulic push, and hammer coring methods in comparison to the quantitative pit across a range of RF. We found the three coring methods (rotary, hydraulic push, and hammer) generated significantly lower estimates of total RF relative to the quantitative pit at sites RF 0.14, RF 0.21, and RF 0.24 (Table 1.2). Analysis of variance showed the fixed effects of site, sampling method, and the interaction between field and sampling method were all highly significant ($p < 0.0001$).

The effect of core diameter can be seen clearly in the distribution of RF by size class for each sampling method (Figure 1.2). The rotary corer has the largest diameter of the coring methods (i.d. = 101.6 mm) and came closest to the pit estimate of total RF at the three rocky sites, but, relative to the pit, still underestimated the >38-mm and the 12-38-mm RF size classes at all of the rocky sites. This was somewhat surprising given that the diameter of the core is greater than 38 mm, and that diamond-tipped bit of this corer is capable of shearing through RF. This finding suggests that corer bias against RF is not only a function of core diameter, but also of relative elementary area, the theoretical minimum sample area necessary for collecting a representative sample in heterogeneous media, such as RF in soil (Buchter et al., 1994). Comparing RF estimates between the rotary core and the pit on an equal area basis may be

necessary to assess whether the diamond-tipped cutting bit is truly effective in eliminating bias against RF.

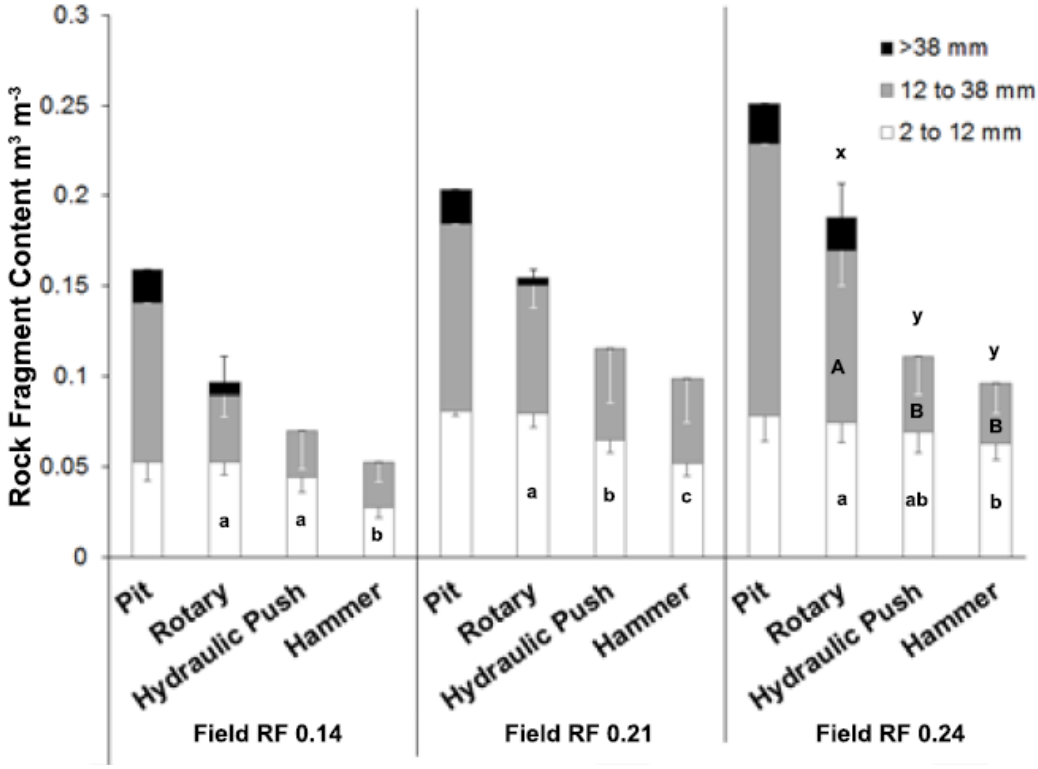

Figure 1.2 Size class distribution of rock fragments (RF) at the 0.24, 0.21, and 0.14 m^3 m^{-3} RF sites. RF size classes are: 2- to 12-mm; 12- to 38-mm, and >38-mm. Lowercase *a* and *b* signify significant differences ($p < 0.05$) for 2- to 12-mm size class; uppercase *A* and *B* for 12- to 38-mm size class, and lowercase *x* and *y* for the >38-mm size class. Quantitative pit data not included in 2- to 12-mm, 12- to 38-mm or >38-mm size class comparisons as only one replicate per size class was analyzed. Error bars are one standard deviation.

The diameters of the hammer (i.d. = 30.0 mm) and hydraulic push (i.d. = 38.1 mm) corers are ≤38 mm, therefore none of the RF in this size class were captured by these methods. At the rockiest site (RF 0.24), the hammer and hydraulic push methods captured significantly less of the RF in the 12-38-mm size class compared to the rotary corer (Figure 1.2). The hammer method also generated significantly lower estimates for the 2-12-mm size class than either the hydraulic push or rotary coring methods at RF 0.14 and RF 0.21 (Figure 1.2). The clear bias of core

diameter in capturing soil RF content is apparent, yet the expected increase in fine-earth soil mass that would be expected from the exclusion or avoidance of RF was not consistently observed, as can be seen from the BD data (Table 1.2).

Coring methods performed better in estimating BD than RF. Rotary core BD was the most similar to pit BD across all sites, while the hammer method tended to have the lowest BD estimates of all methods. The hammer method significantly underestimated $BD_{Hole\text{-}Depth}$ at all sites (RF <0.01, RF 0.14, RF 0.21, and RF 0.24) where pit-BD was 1136, 975, 997, and 891 kg m^{-3}, respectively, and hammer-$BD_{Hole\text{-}Depth}$ was 955, 775, 813, and 778 kg m^{-3}, respectively. The hydraulic push corer also significantly underestimated BD using the hole-depth approach at site RF 0.21, by 127 kg m^{-3} (Table 1.2). Hammer core estimates of $BD_{Core\text{-}Length}$ were closer to pit estimates of BD, and were only significantly different at sites RF <0.01 and RF 0.21, where hammer estimates of $BD_{Core\text{-}Length}$ were 1012 and 890 kg m^{-3}, respectively (Table 1.2). In contrast, the core-length approach did not consistently improve BD estimates with the hydraulic push corer, relative to the hole-depth approach, and lead to overestimates of BD at sites RF 0.14 and RF 0.24 (Table 1.2).

The tendency for the hammer corer to underestimate BD was not limited to the rocky sites, suggesting a strong effect of driving mechanism in addition to exclusion of soil due to obstruction by RF. This is also supported by the lack of significant differences in BD estimates made by the other coring methods with different driving mechanisms at the less rocky sites (RF <0.01 and RF 0.14). The results of this study are consistent with earlier studies that reported low BD estimates with hammer coring in rocky soils (Tuttle et al., 1984; Andraski, 1991), attributed to increased vibration and consequent core loosening. However, our findings suggest that this phenomenon should also be considered in non-rocky soils.

Table 1.2 Estimates of soil physical properties from pit, rotary, hydraulic push and hammer methods at the <0.01, 0.14, 0.21, 0.24 m^3m^{-3} rock fragment sites. †

Site	Sample Method	N	Rock Fragments		Hole Depth		Core Length‡		$BD_{Hole-Depth}$		$BD_{Core-Length}$	
			Mean	CV	Mean	CV	Mean	CV	Mean	CV	Mean	CV
			$m^3\ m^{-3}$	%	m	%	m	%	$kg\ m^{-3}$	%	$kg\ m^{-3}$	%
RF 0.24	Pit	3	0.24a	10	0.291	2	-	-	891ab	6	891§	6
	Rotary	9	0.19b	20	0.298	3	-	-	894a	11	894§	11
	Hydraulic Push	9	0.13c	19	0.297	4	0.260	7	844ab	10	965	6
	Hammer	9	0.11c	19	0.297	8	0.259	5	778b	12	891	8
RF 0.21	Pit	3	0.21a	7	0.290	2	-	-	997a	2	997§	2
	Rotary	9	0.15b	11	0.304	2	-	-	996a	5	996§	5
	Hydraulic Push	9	0.13c	28	0.301	1	0.270	5	870b	10	969	7
	Hammer	9	0.12c	28	0.329	1	0.288	7	813b	13	928	7
RF 0.14	Pit	3	0.14a	17	0.289	2	-	-	975a	9	975ab§	9
	Rotary	9	0.1b	18	0.303	1	-	-	934a	11	934b§	11
	Hydraulic Push	9	0.07c	30	0.303	6	0.290	5	988a	17	1025a	11
	Hammer	9	0.06c	29	0.313	3	0.272	7	775b	12	890b	6
RF <0.01	Pit	3	<0.01	39	0.282	3	-	-	1136a	4	1136a§	4
	Rotary	9	<0.01	99	0.302	2	-	-	1089a	6	1089a§	6
	Hydraulic Push	9	<0.01	229	0.301	4	0.302	5	1106a	6	1102a	6
	Hammer	9	<0.01	162	0.332	1	0.313	1	955b	7	1012b	7

† Different letters indicate that means within a site are significantly different ($p < 0.05$).

‡ Core length = length of extracted soil core. Core-length data are not available for the pit and rotary methods as intact cores cannot be collected with these methods.

§ Pair-wise comparisons of $BD_{Core-Length}$ from the hammer and hydraulic push corers were made with $BD_{Hole-Depth}$ estimates for the pit and rotary corer.

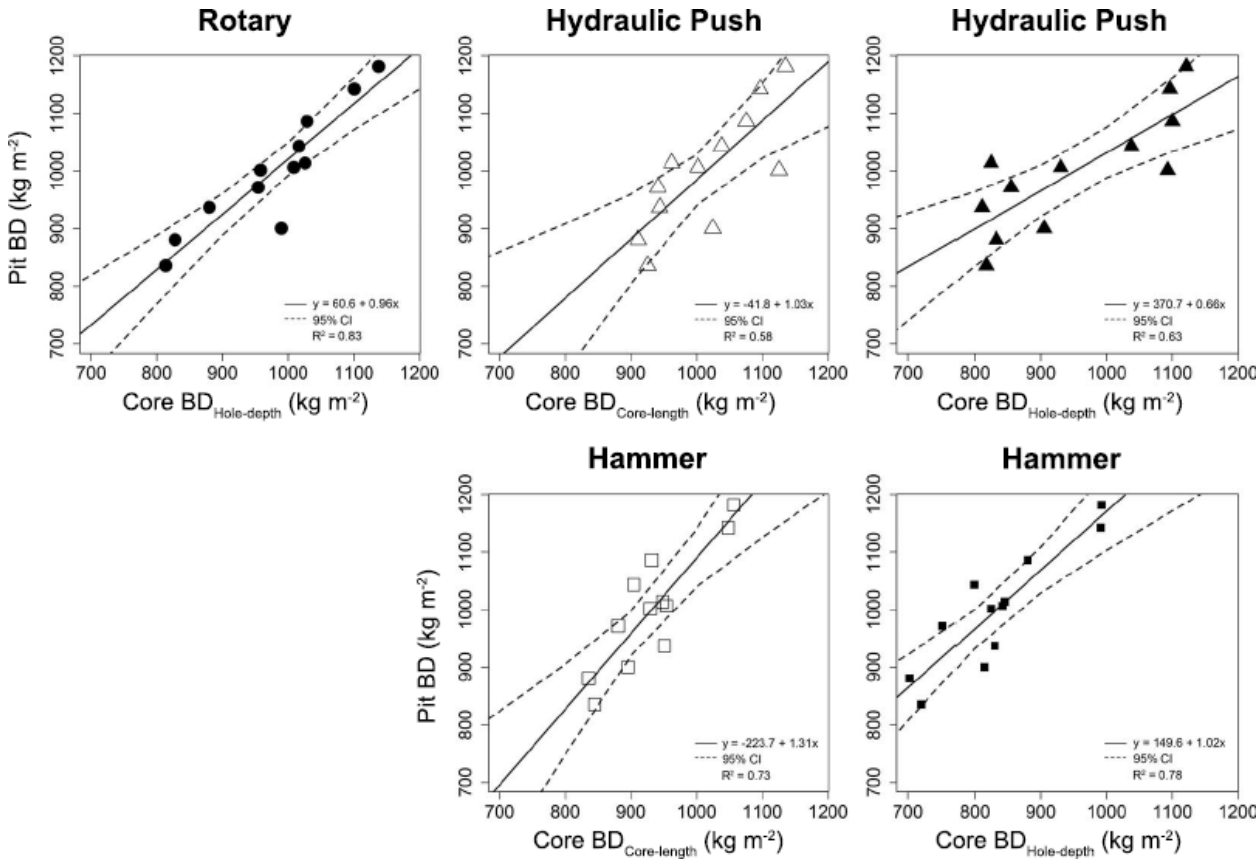

Figure 1.3 Bulk density (BD) of quantitative pit predicted by rotary, hydraulic push, and hammer methods for all sites. $BD_{Core\text{-}Length}$ data shown with open symbols, $BD_{Hole\text{-}Depth}$ data shown with closed symbols. Data for coring methods were averaged by plot.

One solution to the problem of underestimating BD with coring methods is to correct biased BD estimates using BD and RF data from a subset of samples taken with the pit (or other methods known to be more reliable) and a simple linear regression model (Figure 1.3). This is the approach recommended by Kulmatiski et al. (2003), who found that fine earth BD estimates from cores were on average 19% lower than pit estimates for a soil with approximately 0.30 m^3 m^{-3} RF (n = 18). The simple linear regression models used to correct BD for each of the coring methods and calculation approaches with BD data from the pit method were all significant ($p < 0.05$). Slopes for hammer $BD_{Hole\text{-}Depth}$, hydraulic push $BD_{Core\text{-}Length}$ and the rotary method were closest to 1.00 (1.02, 1.03, and 0.96, respectively); and y-intercepts for the latter two models

were closest to 0.00: -41.8 (hydraulic push $BD_{Core\text{-}Length}$), and 60.6 (rotary). These parameter estimates suggest that these methods were less biased than the other methods. The coefficient of determination (R^2) ranged from 0.58 (hydraulic push, $BD_{Core\text{-}Length}$) to 0.83 (rotary) (Figure 1.3). Even though the $BD_{Core\text{-}Length}$ values were closer to the pit BD values overall, the modeled values from hammer and hydraulic push methods using $BD_{Hole\text{-}Depth}$ explained more of the variance in the data than $BD_{Core\text{-}Length}$. The poor fit for the regression models with the hydraulic push method could be due to the relatively small number of samples (n = 12), but based on the results from this study, we would not recommend the regression approach for this method.

The simple regression approach could be used for SOC stock assessments made with multiple sampling methods, for example, if BD sampling was conducted with pits, while additional OC sampling was conducted using a coring method in order to increase spatial coverage for a site and minimize the cost of sampling. The multiple sampling method approach is recommended by Don et al. (2007), who suggest that SOC assessment consist of 56-67% of total samples collected be for OC measurement and 33-44% of the samples collected be for BD measurement. Correcting core estimates of BD with pit data in this scenario could be used to better characterize spatial variability in BD.

No carbonates were detected with the effervescence test, so total C values were reported as OC. No significant difference in OC content for 0-0.30 m was observed between the pit and coring methods at any of the sites, but significant differences were detected between coring methods at sites RF 0.14 and RF 0.21 (Table 1.3). However, estimates of OC were not consistently higher or lower with any particular sampling method across all sites, suggesting that differences are likely due to spatial variability rather than sampling method. This is supported by the lack of significant difference between coring methods and the pit method, and the fact that

Table 1.3 Estimates of soil organic carbon concentration and stocks by pit, rotary, hydraulic push, and hammer methods at the <0.01, 0.14, 0.21, 0.24 m^3m^{-3} rock fragment sites.

			Organic Carbon		**$SOC_{Hole-Depth}$**		**$SOC_{Core-Length}$†**		**$SOC_{Mass-Based}$**	
Site	Sample Method	N	Mean	CV	Mean	CV	Mean	CV	Mean	CV
			kg kg^{-1}	%	kg m^{-2}	%	kg m^{-2}	%	kg m^{-2}	%
RF 0.24	Pit	3	0.0130	4	3.47	2	3.47	2	3.48	4
	Rotary	9	0.0126	7	3.36	7	3.36	7	3.38	7
	Hydraulic Push	9	0.0128	4	3.23	10	3.69	6	3.41	4
	Hammer	9	0.0129	6	3.02	11	3.44	9	3.41	6
RF 0.21	Pit	3	0.0194ab	8	5.79a	6	5.79a	6	5.75	7
	Rotary	9	0.0188b	6	5.61a	7	5.61ab	7	5.60	6
	Hydraulic Push	9	0.0200a	7	5.23a	13	5.82a	8	5.96	7
	Hammer	9	0.0194b	11	4.59b	14	5.24b	8	5.59	9
RF 0.14	Pit	3	0.0303ab	10	8.81a	5	8.81a	5	8.83	9
	Rotary	9	0.0306a	8	8.65a	9	8.54a	9	8.86	8
	Hydraulic Push	9	0.0295b	8	8.54a	13	8.99a	6	8.64	7
	Hammer	9	0.0289b	6	6.71b	10	7.71b	4	8.36	6
RF <0.01	Pit	3	0.0171	14	5.80a	10	5.80	10	5.86	15
	Rotary	9	0.0172	9	5.59a	5	5.59	5	5.86	9
	Hydraulic Push	9	0.0166	10	5.49a	10	5.47	8	5.65	10
	Hammer	9	0.0167	13	4.74b	8	5.03	8	5.77	12

† $SOC_{Hole-Depth}$ data were used for pair-wise comparisons with the pit and rotary methods as core-length measurements cannot be made with these methods. Different letters indicate that means within a site are significantly different ($p < 0.05$).

coring methods were more distant in space from one another than from the pit (Figure 1.1). At RF 0.14, the difference is likely also in part due to heterogeneous spatial distribution of OC related to high rates of manure application (Bocchi et al., 2000). Alternatively, the difference between the rotary method and the hammer and hydraulic push methods at RF 0.14 could be due to a concentration effect whereby equal amounts of organic matter input are incorporated into a smaller volume of fine-earth soil in high rock zones (Bornemann et al., 2011), where RF may have prevented sampling with smaller diameter corers. While this may have occurred at RF 0.14, the data from RF 0.21 and RF 0.24 do not support this hypothesis.

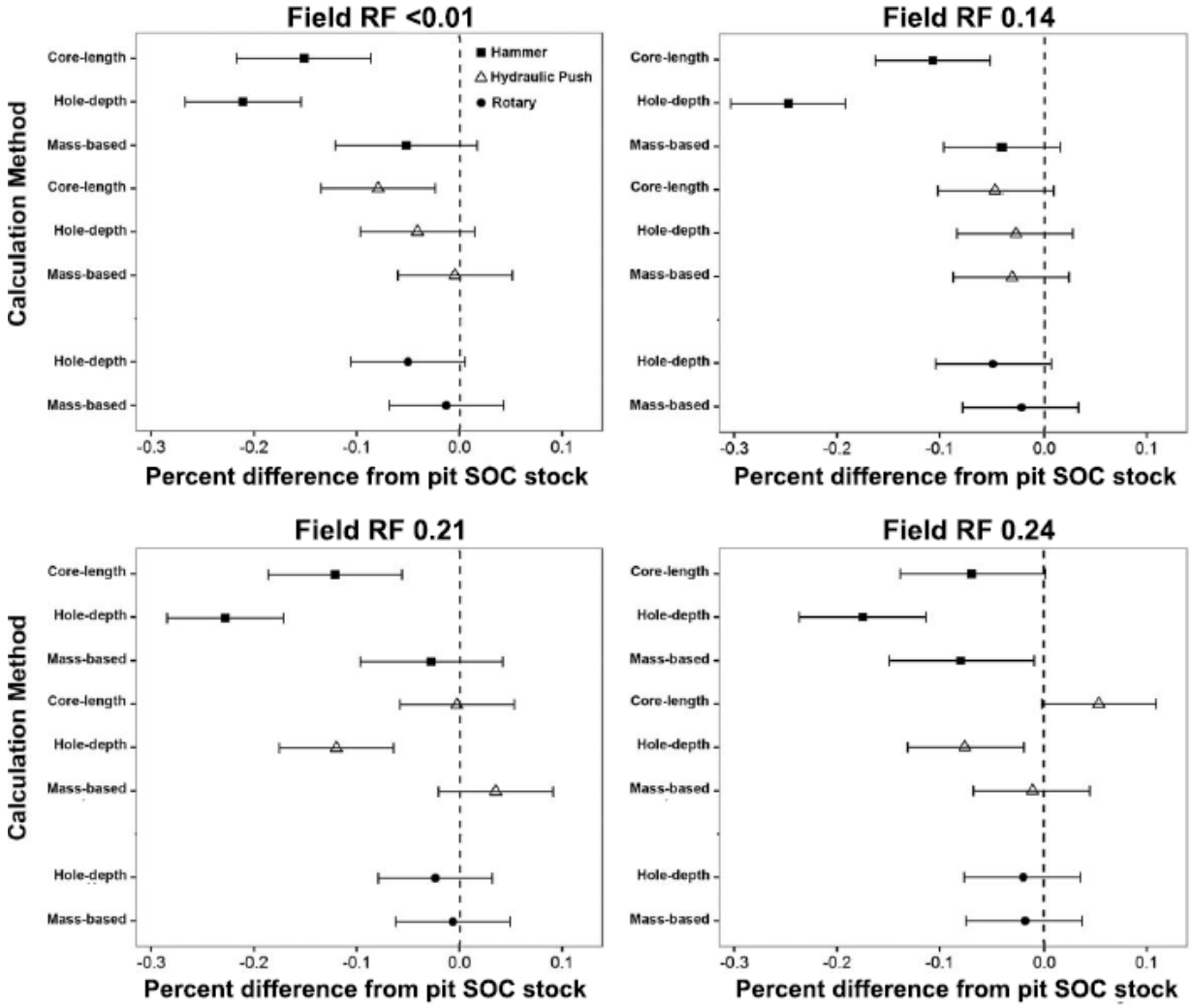

Figure 1.4 Difference in soil organic carbon (SOC) stocks between the quantitative pit versus hammer, hydraulic push, and rotary coring methods as estimated by fixed-depth, and mass-based approaches for the 0.24, 0.21, 0.14, and <0.01 $m^3 m^{-3}$ RF sites. Core-length data are not shown for the pit and rotary methods as intact cores cannot be collected with these methods. Error bars are 95% confidence intervals.

1.3.2. Sampling Method and Calculation Approach on Estimates of SOC Stocks

Analysis of SOC stocks showed site, sampling method, and calculation method were all significant effects, as were the interactions between site and sampling method, and sampling method and calculation method ($p < 0.0001$). However, we found fewer significant differences between pit and coring method estimates of SOC stocks than estimates of BD and RF, even for the rockier sites. One possible explanation for this could be a compensatory effect of underestimating both BD and RF with coring methods. In a comparison of pit and coring methods for rocky forest soils, Xu et al. (2016) also noted that the interdependence of BD, RF, and OC could have a counter-balancing effect: they found significant differences in estimates of BD and RF between pits and cores, but found no significant differences in SOC stocks. We expected that coring methods, which underestimated RF content, would overestimate SOC stocks. However, SOC stock estimates between pit and coring methods were only significantly different with the hammer method (Table 1.3). Relative to the pit, the hammer method significantly underestimated SOC stocks with the hole-depth approaches at sites RF <0.01, RF 0.14, and RF 0.21, and at sites RF 0.14 and RF 0.21 with the core-length approach. Pit-SOC stocks at RF <0.01, RF 0.14, and RF 0.21 were 5.80, 8.81, and 5.79 kg C m^{-2}, while hammer $SOC_{Hole\text{-}Depth}$ stocks were 4.74, 6.71, and 4.59 kg C m^{-2}, and hammer $SOC_{Core\text{-}Length}$ stocks were at RF 0.14 and RF 0.21 were 7.71 and 5.24 kg C m^{-2} (Table 1.3).

Our second study objective was to compare and quantify the effect of sampling method and soil RF content on SOC stock estimates made with fixed-depth versus mass-based calculation approaches. The interaction between calculation approach and site was not significant when comparing absolute differences in SOC stock estimates between pit and coring methods, but was significant when comparing normalized differences ($p < 0.05$) (Figure 1.4).

Analysis of calculation approach in this comparison shows that mass-based estimates from coring methods were generally closer to pit estimates than the fixed-depth estimates, and were only significantly different from pit estimates for the hammer method at site RF 0.24 (Figure 1.4). Normalized differences from the pit were not significant for the rotary core method at any of the sites, but we detected significant differences for the hydraulic push corer at RF 0.21 and RF 0.24 with the hole-depth approach, and at RF <0.01 and RF 0.24 with the core-length approach. Additional significant differences with the hammer method were also seen for the hole-depth approach at RF 0.24 and for the core-length approach at RF <0.01 (Figure 1.4). These results, taken together with hole-depth, core-length, and BD measurements (Table 1.2), provide evidence that RF likely prevent soil from entering the hammer and hydraulic push corers when used in rocky sites. This suggests that the bias introduced by coring methods when estimating SOC stocks is primarily due to poor estimates of soil BD and RF content, and that a mass-based approach may be an appropriate tool for improving SOC stock assessments that rely on corers.

SOC stocks were also calculated using BD values generated by regression against pit BD (data not shown). This fixed-depth approach greatly improved hammer coring estimates of SOC stocks, with the only significant difference among sampling methods at RF 0.14 where hammer $SOC_{Hole\text{-}Depth}$ was 8.20 kg C m^{-2} and hydraulic push $SOC_{Core\text{-}Length}$ was 9.07 kg C m^{-2} ($p = 0.018$).

1.3.3. Sources of Error in SOC Stock Calculations

Comparing the relative sources of error in SOC stock calculations shows that on average BD contributed more to the overall error (5 to 82%) at the rocky sites (RF 0.14, RF 0.21, and RF 0.24) than at RF <0.01 (5 to 31%), where OC was the most important source of variance for all methods (9 to 74%) (Figure 1.5). Fixed-depth SOC stock estimates using the hole-depth approach with the hydraulic push and hammer coring methods were more variable on average at

RF 0.14, RF 0.21, and RF 0.24 compared to the pit and rotary coring methods (Table 1.3). At RF 0.14, RF 0.21, and RF 0.24, $BD_{Hole\text{-}Depth}$ contributed more relative variance to SOC stocks than $BD_{Core\text{-}Length}$ for these methods (Figure 1.5), while the relative contribution of OC, BD, and covariance of OC and BD (OC-BD) is more equal across sampling methods and calculation approaches at the less rocky sites RF 0.14 and RF <0.01, in comparison to RF 0.21 and RF 0.24. A negative covariance between BD and OC was observed at most sites (Figure 1.5), which follows from the inverse relationship between organic matter and BD (Adams, 1973; Arvidsson, 1998). This negative covariance reduces SOC stock variance, and has been reported by other authors as well (Goidts et al., 2009; Schrumpf et al., 2011; Xu et al., 2015). At the RF 0.21 and RF 0.24 sites, the pit method had the largest negative covariance of OC-BD, while at RF 0.21 $OC\text{-}BD_{Hole\text{-}Depth}$ for the hydraulic push method had a positive covariance between these terms (Figure 1.5).

Since our method of calculating BD in this study incorporates the error of the RF term, our results are in line with the finding in Schrumpf et al. (2011), who reported that the dominant source of measured SOC stock variability for non-rocky soils was OC, but that as RF content increased, RF became the primary source of variability. Similarly, Goidts et al. (2009) identified RF content as the primary source of SOC stock variability at the field scale for croplands with high RF content.

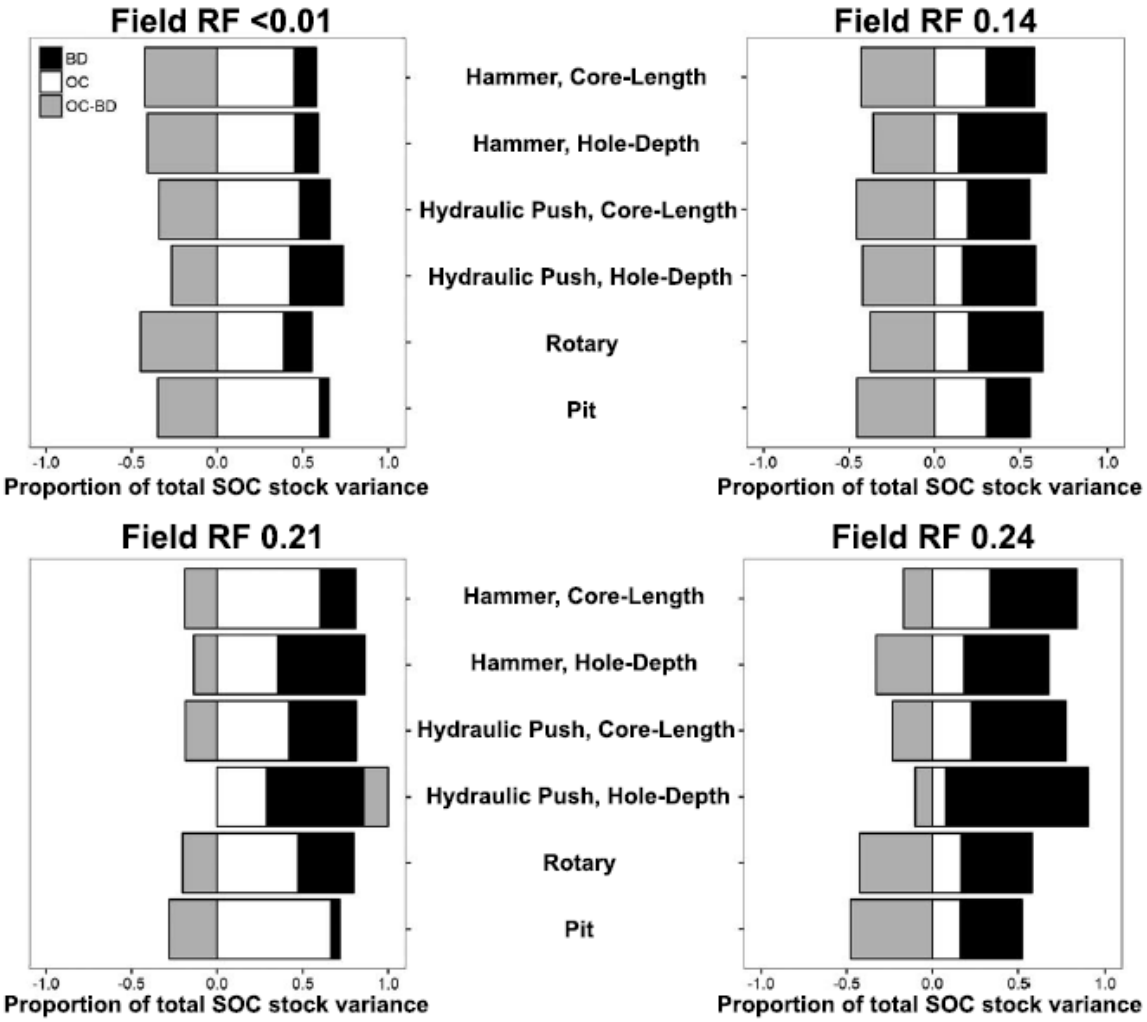

Figure 1.5 Relative contribution (%) of soil organic carbon (SOC) stock parameters [OC concentration (OC), soil bulk density (BD), OC and BD covariance (OC-BD)] to total variance of SOC stocks. Core-length data are not shown for the pit and rotary methods as intact cores cannot be collected with these methods.

1.3.4. Cost Analyses

Our third objective was to assess how soil RF content and sampling equipment affected the cost of sample collection and laboratory analysis for the rockiest and least rocky sites (RF 0.24 and RF <0.01). Sampling in rocky soils was more costly than sampling in non-rocky soils, but the relationship between the cost of sampling and soil RF content varied by sampling method (Table 1.4). The main differences in cost are due to the difference in time required for sample collection, and from both fixed and variable equipment costs. In particular, fixed equipment costs

varied by an order of magnitude between sampling methods, from US $776 (pit) to US $23,800 (hydraulic push).

Table 1.4 Comparison of sampling costs at the <0.01 and 0.24 m^3m^{-3} rock fragment sites

	Field Rock Fragment Concentration				
	$m^3\ m^{-3}$				
	<0.01			0.24	
Sampling Method	**Fixed Equipment Cost†**	**Sample Collection Time‡**	**Variable Sampling Cost§**	**Sample Collection Time**	**Variable Sampling Cost**
	$	Minutes	$	minutes	$
Pit	776.18	360.0	99.57	400.0	109.57
Rotary	1511.73	22.1	14.90	29.3	16.69
Hydraulic Push	23800.53	9.7	11.23	23.4	14.65
Hammer	5100.75	10.2	16.13	19.5	18.45

† Fixed equipment cost included all overhead costs.
‡ Sample collection time was defined on a per sample basis, in person-hours.
§ Variable sampling cost was defined on a per sample basis, and included the cost of labor required for sample collection and laboratory analysis, as well as disposable equipment used for sample collection, such as liner tubes and sealable plastic bags.

The total variable per sample cost decreased in the following order: pit > hammer > rotary > hydraulic push at both RF24 and RF<1 (Table 1.4). The variable sampling cost estimated for the quantitative pit, approximately 100 USD, was more than seven times as costly on average when compared to the three coring methods, suggesting that it would be prohibitively expensive to collect a large number of samples with the pit method. Sample processing costs were similar for all methods, and for the coring methods they were also notably greater than the cost of sample collection (not shown). The increase of variable sampling costs between the <0.01 and 0.24 $m^3\ m^{-3}$ RF sites was less substantial for the rotary coring method (~19%) than for the hydraulic push and hammer methods (~82 and 63%, respectively). While the hydraulic push corer has the lowest variable sampling cost at both sites, this cost is similar for all three coring methods at RF 0.24, suggesting that while still more time-consuming to operate, the rotary corer

becomes more cost-competitive at rockier sites. Although not included in this analysis, if equipment were rented, the cost of rental would be expected to increase in relation to the sample collection time, which could influence coring method selection (Singh et al., 2013).

1.4. CONCLUSIONS AND RECOMMENDATIONS FOR SAMPLING IN ROCKY SOILS

Understanding the potential bias introduced by sampling equipment, and the relationship between sampling method, soil RF content, and associated costs of sample collection and analysis is critical for both improving accuracy and reducing uncertainty in SOC stock assessments in rocky agricultural soils. Based on the results of this study, the optimal coring method for SOC stock assessment in rocky sites is the rotary diamond-tipped corer. Estimates of BD, RF content, and SOC stocks made with this method were generally more accurate than standard coring methods, relative to the quantitative pit, and the per sample cost was similar to the other coring methods. Hydraulic push corers would be the next choice based on the same criteria, while hammer corers are the least recommended approach for rocky soils as this method had a higher probability of producing biased estimates (Tables 1.2, 1.3, and Figure 1.4).

Estimates of SOC stock made with common coring methods such as the hydraulic push and hammer methods tested in this study tend to underestimate RF and BD at rocky sites, as well as SOC stocks when calculated with the standard fixed-depth (hole-depth) approach. If sampling methods that are less expensive or destructive than quantitative pits are needed, then the site-specific regression approach to correcting BD data collected with the hydraulic push and hammer methods showed promise in this study. However, this approach requires an existing calibration data set from a more reliable sampling method, and additionally, as sample numbers were limited, this approach requires further testing. If using multiple sampling methods, this

study provides support for an approach in which OC samples could be collected with the hydraulic push or hammer methods to increase spatial coverage of a site, as no sampling method bias was detected in OC determination, and the quantitative pit or possibly the rotary coring method could be used to establish an appropriate reference mass for calculating SOC stocks.

Our results show that using a mass-based approach improves reliability of SOC stock estimates on rocky soils and further support the recommended approach in SOC stock assessment to report SOC stocks on a mass-basis. For monitoring SOC stocks in rocky soils, we suggest that 1) soil references mass are set with either the quantitative pit or rotary core method, 2) sampling equipment and SOC stock calculation method are taken into account when comparing BD, RF, and SOC stocks, and 3) the hammer method be avoided, unless additional BD samples are collected with a more reliable method. In cases where hammer coring is the only practical option, then the stocks should be reported on a mass-basis, with reference masses set with a more reliable method, such as quantitative pit sampling, in order to limit the potential for bias. We also note that as our study focused on sampling surface horizons to a 0.3-m depth, we recommend further evaluation of the effect of mass-based SOC stock calculation and sampling method when estimating SOC stocks for soil profiles below 0.3-m in depth, on both rocky and non-rocky soils.

1.5. REFERENCES

Adams, W.A. 1973. The effect of organic matter on the bulk and true densities of some uncultivated podzolic soils. J. Soil Sci. 24(1): 10–17.

Adhikari, K., A.E. Hartemink, B. Minasny, R. Bou Kheir, M.B. Greve, and M.H. Greve. 2014. Digital mapping of soil organic carbon contents and stocks in Denmark. PLoS One 9(8): e105519.

Andraski, B.J. 1991. Balloon and core sampling for determining bulk density of alluvial desert soil. Soil Sci. Soc. Am. J 55: 1188–1190.

Arvidsson, J. 1998. Influence of soil texture and organic matter content on bulk density, air content, compression index and crop yield in field and laboratory compression experiments. Soil Tillage Res. 49(1-2): 159–170.

Bocchi, S., A. Castrignano, F. Fornaro, and T. Maggiore. 2000. Application of factorial kriging for mapping soil variation at field scale. Eur. J. of Agron. 13(4): 295—308.

Bornemann, L., M. Herbst, G. Welp, H. Vereecken, and W. Amelung. 2011. Rock fragments control size and saturation of organic carbon pools in agricultural topsoil. Soil Sci. Soc. Am. J. 75(5): 1898-1907.

Buchter, B., C. Hinz, and H. Flühler. 1994. Sample size for determination of coarse fragment content in a stony soil. Geoderma 63(3-4): 265–275.

CAST (Council for Agricultural Science and Technology). 2011. Carbon sequestration and greenhouse gas fluxes in agriculture: challenges and opportunities. Task Force Report 142, Council for Agricultural Sciences and Technology, Ames, Iowa, 117 pp.

Conant, R.T., S.M. Ogle, E.A. Paul, and K. Paustian. 2011. Measuring and monitoring soil organic carbon stocks in agricultural lands for climate mitigation. Front. Ecol. Environ. 9(3): 169–173.

Don, A., J. Schumacher, M. Scherer-Lorenzen, T. Scholten, and E.-D. Schulze. 2007. Spatial and vertical variation of soil carbon at two grassland sites — Implications for measuring soil carbon stocks. Geoderma 141(3-4): 272–282.

Ellert, B.H., and J.R. Bettany. 1995. Calculation of organic matter and nutrients stored in soils under contrasting management regimes. Can. J. Soil Sci. 75(4): 529–538.

Ellert, B.H., H.H. Janzen, and B.G. McConkey. 2001. Measuring and comparing soil carbon storage. *In*: R. Lal, R., J.M. Kimble, R.F. Follett, and B.A. Stewart (Eds.), Assessment Methods for Soil Carbon. Lewis Publishers, Boca Raton, FL, pp. 131–144.

Gifford, R.M., and M.L. Roderick. 2003. Soil carbon stocks and bulk density: Spatial or cumulative mass coordinates as a basis of expression? Glob. Chang. Biol. 9(11): 1507–1514.

Goidts, E., B. Van Wesemael, and M. Crucifix. 2009. Magnitude and sources of uncertainties in soil organic carbon (SOC) stock assessments at various scales. Eur. J. Soil Sci. 60(5): 723–739

Harrison, R.B., A.B. Adams, C. Licata, and B. Flaming. 2003. Quantifying deep-soil and coarse-soil fractions : Avoiding sampling bias. Soil Sci. Soc. Am. J 67(5): 1602-1606.

Hedley, C.B., I.J. Payton, I.H. Lynn, S.T. Carrick, T.H. Webb, and S. McNeill. 2012. Random sampling of stony and non-stony soils for testing a national soil carbon monitoring system. Soil Res. 50(1): 18–29.

Hoffmann, U., T. Hoffmann, E. Johnson, and N.J. Kuhn. 2014. Assessment of variability and uncertainty of soil organic carbon in a mountainous boreal forest (Canadian Rocky Mountains, Alberta). Catena 113: 107–121

Intergovernmental Panel on Climate Change (IPCCC). 2006. Guidelines for national greenhouse gas inventories. Vol. 4. Agriculture, forestry and other land uses. Available at www.ipcc-nggip.iges.or.jp/public/2006gl/vol4.htm (verified 15 July 2015). Inst. for Global Environ. Strategies, Hayama, Japan.

Johnson, D.W., C.F. Hunsaker, D.W. Glass, B.M. Rau, and B.A. Roath. 2010. Carbon and nutrient contents in soils from the Kings River Experimental Watersheds, Sierra Nevada Mountains, California. Geoderma 160(3-4): 490–502.

Kimble, J.M., R.B. Grossman, and S.E. Samson-Liebig. 2001. Methodology for sampling and preparation for soil carbon determination. *In*: R. Lal, J.M. Kimble, R.F. Follett, and B.A. Stewart, editors, Assessment Methods for Soil Carbon. Lewis Publishers, Boca Raton, FL. p. 15–30.

Kulmatiski, A., D.J. Vogt, T.G. Siccama, and K.H. Beard. 2003. Detecting nutrient pool changes in rocky forest soils. Soil Sci. Soc. Am. J 67: 1282–1286.

Lal, R. 2009. Challenges and opportunities in soil organic matter research. Eur. J. Soil Sci. 60(2): 158–169.

Lee, J., J.W. Hopmans, D.E. Rolston, S.G. Baer, and J. Six. 2009. Determining soil carbon stock changes: Simple bulk density corrections fail. Agric., Ecosyst. Environ. 134: 251-256.

Levine, C.R., R.D. Yanai, M. a. Vadeboncoeur, S.P. Hamburg, A.M. Melvin, C.L. Goodale, B.M. Rau, and D.W. Johnson. 2012. Assessing the Suitability of Rotary Coring for Sampling in Rocky Soils. Soil Sci. Soc. Am. J. 76(5): 1707

Mäkipää, R., M. Hakkinen, P. Muukkonen, and M. Peltoniemi. 2008. The costs of monitoring changes in forest soil carbon stocks. Boreal Environ. Res. 13(November): 120–130.

Mathieu, J.A., C. Hatté, J. Balesdent, and É. Parent. 2015. Deep soil carbon dynamics are driven more by soil type than by climate: a worldwide meta-analysis of radiocarbon profiles. Glob. Chang. Biol.

Mehler, K., I. Schöning, and M. Berli. 2014. The importance of rock fragment density for the calculation of soil bulk density and soil organic carbon stocks. Soil Sci Soc. Am. J 78: 1186–1191.

Miller F.T., and R.L. Guthrie. 1984. Classification and distribution of soils containing rock fragments in the United States. *In*: J.D. Nichols, P.L. Brown, and W.J. Grant, editors, Erosion and Productivity of Soils Containing Rock Fragments. Soil Science Society of America, Madison, WI. p. 1-6.

Minasny, B., A.B. McBratney, B.P. Malone, and I. Wheeler. 2013. Digital Mapping of Soil Carbon. Adv. Agron. 118: 1-47.

Neeley, J.A. 1965. Soil survey: Tompkins County, New York. Series 1961, no. 25. USDA, Soil Conserv. Serv., Gov. Print. Office, Washington, DC.

Page-Dumroese, D.S., R.E. Brown, M.F. Jurgensen, and G.D. Mroz. 1999. Comparison of Methods for Determining Bulk Densities of Rocky Forest Soils. Soil Sci. Soc. Am. J. 63(2): 379.

Poesen, J., and H. Lavee. 1994. Rock fragments in top soils : significance and processes. Catena 23: 1–28.

Press, W.H., S.A. Teukolsky, W.T. Vetterling, and B.P. Flannery. 2007. Numerical recipes: The art of scientific computing. 3rd ed. Cambridge University Press, New York.

R. 2013. R: A language and environment for statistical computing. *In:* R.C. Team, editors. Vienna, Austria: Foundation for Statistical Computing.

Rau, B.M., A.M. Melvin, D.W. Johnson, C.L. Goodale, R.R. Blank, G. Fredriksen, W.W. Miller, J.D. Murphy, D.E. Todd, and R.F. Walker. 2011. Revisiting soil carbon and nitrogen sampling. Soil Sci. 176(6): 273–279.

Rovira, P., T. Sauras, J. Salgado, and A. Merino. 2015. Towards sound comparisons of soil carbon stocks: A proposal based on the cumulative coordinates approach. Catena 133:420-431.

Rumpel, C., and I. Kögel-Knabner. 2011. Deep soil organic matter-a key but poorly understood component of terrestrial C cycle. Plant Soil 338(1): 143–158.

Rytter, R.M. 2012. Stone and gravel contents of arable soils influence estimates of C and N stocks. Catena 95: 153–159.

Schmidt, M.W.I., M.S. Torn, S. Abiven, T. Dittmar, G. Guggenberger, I. a. Janssens, M. Kleber, I. Kögel-Knabner, J. Lehmann, D. a. C. Manning, P. Nannipieri, D.P. Rasse, S. Weiner, and S.E. Trumbore. 2011. Persistence of soil organic matter as an ecosystem property. Nature 478(7367): 49–56.

Schrumpf, M., E.D. Schulze, K. Kaiser, and J. Schumacher. 2011. How accurately can soil organic carbon stocks and stock changes be quantified by soil inventories? Biogeosciences 8(5): 1193–1212.

Schrumpf, M., K. Kaiser, G. Guggenberger, T. Persson, I. Kögel-Knabner, E.D. Schulze, I. Kogel-Knabner, and E.D. Schulze. 2013. Storage and stability of organic carbon in soils as related to depth, occlusion within aggregates, and attachment to minerals. Biogeosciences 10(3): 1675–1691

Singh, K., B. Murphy, and B. Marchant. 2013. Towards cost-effective estimation of soil carbon stocks at the field scale. Soil Res. 50: 672–684.

Soil Survey Laboratory Staff. 2004. Soil survey laboratory methods manual. Soil Surv. Invest. Rep. 42, Version 4.0. US Gov. Print. Office, Washington, DC.

Syswerda, S.P., T. Corbin, D.L. Mokma, N. Kravchenko, and G.P. Robertson. 2011. Agricultural Management and Soil Carbon Storage in Surface vs. Deep Layers. Soil Sci. Soc. Am. J. 75(1): 92

Throop, H.L., S.R. Archer, H.C. Monger, and S. Waltman. 2012. When bulk density methods matter: Implications for estimating soil organic carbon pools in rocky soils. J. Arid Environ. 77: 66–71.

Tuttle, C.L., M.S. Golden, and D.L. Sirois. 1984. A portable tool for obtaining soil cores in clayey or rocky soils. Soil Sci. Soc. Am. J. 48: 1453–1455.

Vadeboncoeur, M.A., S.P. Hamburg, J.D. Blum, M.J. Pennino, R.D. Yanai, and C.E. Johnson. 2012. The quantitative soil pit method for measuring belowground carbon and nitrogen stocks. Soil Sci. Soc. Am. J. 76(6): 2241-2255.

Vandenbygaart, A.J., 2006. Monitoring soil organic carbon stock changes in agricultural landscapes: issues and a proposed approach. Can. J. Soil Sci. 86:451–463.

Vincent, K.R., and O.A. Chadwick. 1994. Synthesizing bulk density for soils with abundant rock fragments. Soil Sci. Soc. Am. J. 58(2): 455-464.

Wendt, J.W., and S. Hauser. 2013. An equivalent soil mass procedure for monitoring soil organic carbon in multiple soil layers. Eur. J. Soil Sci. 64(1): 58–65.

West, T.O., and W.M. Post. 2002. Soil organic carbon sequestration rates by tillage and crop rotation: A global data analysis. Soil Sci. Soc. Am. J. 66(6): 1930–1946.

Wolfe, D.W. 2013. Contributions to climate change solutions from the agronomy perspective. *In:* D. Hillel and C. Rosenzweig, editors, Handbook of climate change and agroecosystems: Global and regional aspects and implications. Imperial College Press, London. p.11–31.

Wuest, S.B., 2009. Correction of bulk density and sampling method biases using soil mass per unit area. Soil Sci. Soc. Am. J. 73:312–316.

Xu, B., Y. Pan, A.H. Johnson, and A.F. Plante. 2016. Method Comparison for Forest Soil Carbon and Nitrogen Estimates in the Delaware River Basin. Soil Sci. Soc. Am. J. 80(1): 227–237.

Chapter 2: Field-scale assessment of subsoil, topsoil, and profile soil organic carbon stocks

ABSTRACT

Variability of soil organic C (OC) stocks, particularly in the subsoil, remains both a statistical and financial challenge for verifying SOC sequestration goals. Tractor-mounted visible/near-infrared spectrophotometers (VNIR-p) generate high resolution measurements of surface soil organic matter (SOM_v) with the potential to reduce the number of soil core samples needed for mapping and estimating baseline soil OC stocks. We sought to: 1) compare the stratification performance of SOM_v, terrain, and soil survey data with simple random sampling for estimating topsoil (0-300 kg soil m^{-2}, ca. 0-0.30 m), subsoil (300-650 kg soil m^{-2}, ca. 0.30-0.75 m), and profile (0-650 kg soil m^{-2}, ca. 0-0.75 m) OC stocks as a function of sampling intensity; and 2) develop spatially explicit models of topsoil, subsoil, and profile OC stocks using stratification to select minimal calibration samples. Soil cores (n=200) and SOM_v measurements (n=3534) were collected from two 11 ha arable fields in IA, USA with different distributions of soil OC stocks (Field A, Field B). Stratification approaches were compared by the root mean square error (RMSE) of 1000 simulations of resampling. SOM_v outperformed soil survey data, terrain indices, and simple random sampling for topsoil and profile SOC stock, but stratification did not substantially improve subsoil estimates. The best topsoil OC stock model had SOM_v as the sole predictor, with an R^2=0.68 and RMSE=1.31 at Field B, and R^2=0.54 and RMSE=0.97 at Field A. Both SOM_v and terrain indices were useful in the subsoil (R^2=0.32 and RMSE=2.41, averaged across fields) and profile (R^2=0.55 and RMSE=2.41, averaged across fields) soil OC stock models. Due to the greater spatial covariance of soil OC stocks over shorter distances in subsoil compared to topsoil, SOM_v does not adequately capture the distribution of subsoil OC stocks, and future study should target what may drive these distinct patterns of variation.

2.1. INTRODUCTION

Reductions in greenhouse gas emissions must be complimented with increases in negative emissions in order to stabilize atmospheric CO2 concentrations and prevent catastrophic changes in climate (Ciais et al., 2013). In the wake of the 2015 United Nations Climate Change Conference, initiatives such as "4 per mille" have brought soil C sequestration, a low-tech form of negative emissions, into the global public dialog on climate change (Chabbi et al., 2017). Soil C sequestration on arable lands has a high climate change mitigation potential due to the large area over which the approach can be adopted (Paustian et al., 2016), and in addition to the climate change mitigation potential, sequestering C in the form of soil organic matter confers co-benefits such as improvements in agricultural productivity and climate change adaptation capacity, which together enhance food security (Smith et al., 2012; Koch et al., 2013; Wolfe, 2013).

A key challenge for verifying soil C sequestration targets such as 4 per mille is the high variability of soil OC stocks at the field scale. More than half of the global terrestrial soil OC stock is estimated to be in the subsoil (Batjes et al., 1996; Jobbágy and Jackson, 2000), and a recent study assessing the viability of the 4 per mille initiative emphasizes the importance of considering soil OC sequestration to a depth of 1m (Minasny et al., 2017). Yet the distribution of subsoil OC is poorly characterized and the dynamics of soil OC cycling throughout the whole soil profile are not well understood (Rumpel and Kögel-Knabner, 2011; Lehmann and Kleber, 2015).

The heterogeneous distribution of soil OC stocks, in both the vertical and horizontal dimensions, creates statistical as well as financial hurdles for soil OC assessment (Smith et al., 2012; Lacoste et al., 2014; Liu et al., 2016). Stratified sampling is a frequently applied approach

for determining baseline soil OC stocks (Sherpa et al., 2016; Viscarra Rossel et al., 2016), as it lowers the cost of sampling by partitioning the variance of the target variable into relatively homogenous categorical classes, or strata. Consequently, fewer samples are needed to generate an accurate estimate of the global mean than in the simple random sampling case. However, soil OC distribution at the field scale is often characterized by "hot spots" in which soil OC stocks are locally concentrated, suggesting that sampling designs targeted at reducing sample variance may not be appropriate for mapping and monitoring of soil OC stocks (de Gruijter et al., 2006; Allen et al., 2010).

Soil survey maps are commonly used for stratification when conducting soil sampling, but these maps have historically been generated at a resolution that is too coarse for accurate field-scale mapping of heterogeneous soil properties like soil OC stocks (Minasny, et al., 2013). This approach is also insensitive to the effects of recent management. Remote sensing products, such as terrain indices derived from a digital elevation map (DEM), are a free source of high-resolution data that have been widely used both to improve soil OC stock models and to inform soil sampling schemes (Simbahan and Dobermann, 2006; de Gruijter et al., 2016). Proximal sensing, e.g. using a tractor-mounted unit with electromagnetic sensors and visual/near-infrared spectrophotometers is another relatively inexpensive source of high-resolution data for soil properties such as soil organic matter or cation exchange capacity (Bricklemyer and Brown, 2010). A key advantage of proximal sensing technology over remote sensing is the extremely high spatial resolution of the data (Viscarra Rossel et al., 2016), and, although VNIR-p measurements are restricted to the uppermost soil layer, these measurements physically transcend the steep environmental gradient between the atmosphere and the soil, offering a more direct insight into soil properties (Gebbers and Adamchuk, 2010).

Previous studies have shown that topsoil and subsoil OC stocks are well-correlated, but that distinct processes control the dynamics of soil OC cycling in the topsoil and subsoil pools (Hobley et al., 2015; Rumpel et al., 2015; Jague et al., 2016). These findings suggest that sampling and modeling approaches that target only the topsoil, or that treat the whole soil profile as a single pool, may obscure the relationship between subsoil OC stock and potential drivers. Research at the global and regional scales has indicated that subsoil OC dynamics are strongly dependent on mineralogy and soil parent material, in contrast to climatic, biological, and soil management impacts that dominate in the topsoil (Meersmans et al., 2009; Mathieu et al., 2015). Studies at the field scale have confirmed the importance of mineralogy as well as soil structure to subsoil OC dynamics, and have also suggested that spatial heterogeneity of soil OC is greater in the subsoil than in topsoil (Salomé et al., 2010; Schrumpf et al., 2013). Recent recognition that some fractions of subsoil C cycle on decadal and not just centennial or millennial scales (Koarashi, et al. 2012), underscores the need to better understand this important soil C pool. Improving the accuracy of soil OC assessment will require designing sampling schemes that capture the variance in subsoil OC stocks in addition to topsoil OC stocks.

Working under the reality of financial constraints, we need to be able to meet the dual objectives of designing more efficient soil sampling schemes as well as accurately mapping both topsoil and subsoil OC stocks at the field scale. The current study was undertaken to assess the relevance of soil survey, remote sensing, and commercially-provided proximal sensing data as sources for mapping and estimation of baseline subsoil OC stocks, in comparison to topsoil and whole profile soil OC stocks.

Specifically, we sought to:

1) Compare the stratification performance of SOM_v, terrain indices, and soil survey data for estimating mean soil OC stocks for topsoil, subsoil, and whole soil profile as function of sampling intensity.
2) Develop spatially explicit models for topsoil, subsoil, and whole profile soil OC stocks using the best performing stratification approach to select a calibration dataset with minimal direct observations.

2.2. METHODS

2.2.1. Site description

The study was conducted on a commercial farm in Kossuth County, IA, in the USA. Soils were loams developed from glacial till. Two adjacent 11 ha fields with distinct relationships between topsoil and subsoil OC stocks were sampled: Field A, and Field B. The two fields were under different cropping systems for the past 12 years, with the rotation at Field A consisting of maize (*Zea mays*), soybean (*Glycine max*), oat (*Avena sativa*), and alfalfa (*Medicago sativa*), in contrast to a maize/soybean rotation at Field B. Maize and soybean yields were comparable between Field A and Field B. Both sites received liquid hog manure applications of approximately 47 m^3 ha^{-1} during the maize year of the rotation, with supplementary inorganic fertilizer applied to Field B. Both fields were minimally tilled with chisel plowing to a depth of 0.4 m following maize harvest and disc tillage to a depth of 0.1 m prior to planting soybean.

2.2.2. Soil core and proximal sensing data

Soil cores were collected in October 2012 using an equilateral triangular grid design with 42-m spacing; additional offset grid cores were collected at a distance of one meter from one

third of the grid points for a total of 100 cores at Field A and 99 cores at Field B (Figure 2.1). One core from Field B was contaminated in the laboratory, and could not be used in the analysis. Cores were collected with a power hammer driven soil coring apparatus (i.d. 30 mm, JMC Soil Samplers; Newton, IA, USA) to a depth of 0.75 m. VNIR-p data were collected in October 2011 with the Veris mobile sensor platform version 3 (MSP3), fitted with a spectrophotometer (350–2224nm, 8-nm spectral resolution) mounted to a vertical shank and pulled behind a tractor (Veris Technologies Inc., Salina, KS, USA). Spectral measurements were collected at a depth of approximately 0.05 m at a rate of approximately 20 spectra per second (Bricklemyer and Brown, 2010). Measurements were averaged to generate integrated data points at 3-m intervals along transects spaced 20 m apart, yielding a density of 160 data points ha^{-1} (Figure 2.1). Electrical conductivity was measured using paired direct contact electrodes mounted to rolling coulters on the MSP3 unit, and used to predict cation exchange capacity (CEC) (Sudduth et al., 2005). Electrical conductivity readings were collected at a density of 120-140 samples ha^{-1}. Calibration soil cores were collected at a density of 4 samples per ha, and soil organic matter was measured by weight loss on ignition. CEC was measured using the ammonium acetate method. A cross-validated multivariate calibration approach was used to build a prediction model for SOM_v, and spatially explicit predictions of both SOM_v and CEC were provided as part of a commercial service package (Figure 2.2*h*, 2.2*i*). Total cost for the service is estimated at 4-5 USD ha^{-1}. The Veris MSP3 was selected as it has been shown to be one of the highest performing units for precision agriculture (Gebbers et al., 2009; Knadel, et al., 2015), and because this unit is commercially available.

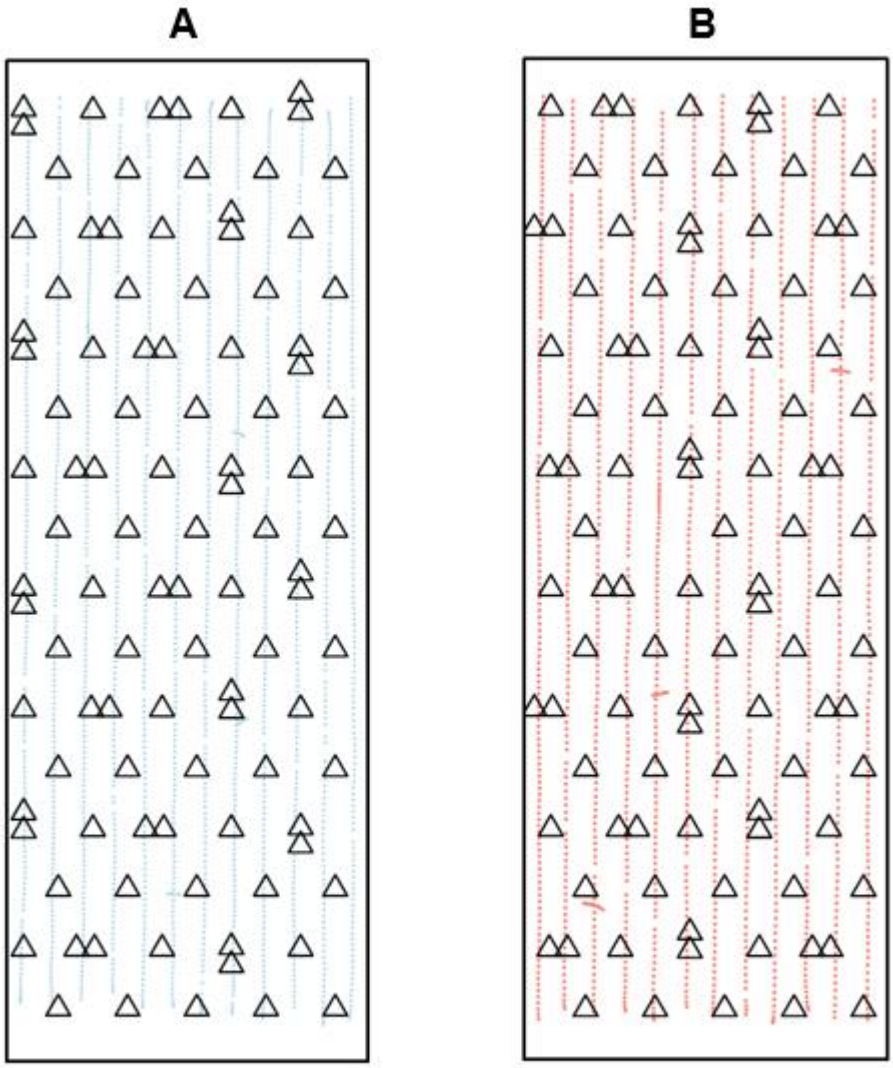

Figure 2.1 Soil core (open triangles) and proximal sensing locations (filled circles) for Field A (**left**) and Field B (**right**). Offset grid point locations for soil cores exaggerated from 1 to 10m for display.

2.2.3. Laboratory analyses

Soil cores were sectioned into five depth increments, 0-0.10 m, 0.10-0.20 m, 0.20-0.30 m, 0.30-0.50 m, and 0.50-0.75 m. Soils were sieved to 2 mm and air-dried at 35C for 48 h in a convection oven. Subsamples of the <2-mm soil were further dried to 105C to determine moisture content and calculate bulk density. Total C concentration was measured on air-dry <2-mm material using dry combustion (Carlo Erba NC2500; Thermo Finnigan, San Jose, CA, USA). Soils were

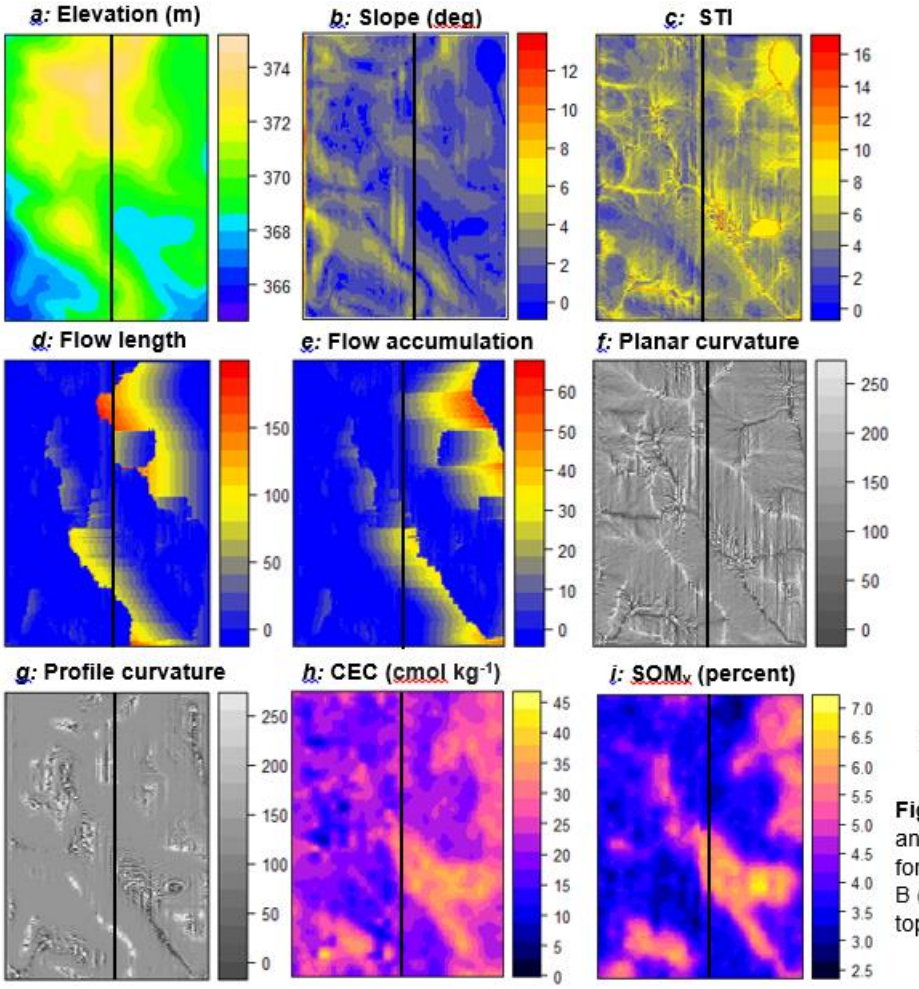

Figure 2.2 Terrain variables (***a-g***) and proximal sensing data (***h-i***), for Field A (***left panels***) and Field B (***right panels***). **STI** = soil topographic wetness index.

screened for carbonates with a qualitative effervescence test using 1M hydrochloric acid (Soil Survey Staff, 2004), and 1:2 $CaCl_2$ pH was measured as well (Soil Survey Staff, 2004). Inorganic C (IC) contents of soils for soils that tested positive for carbonates and had pH > 6.5 were estimated with diffuse reflectance mid-infrared Fourier transform spectroscopy (MIR). Subsamples of <2-mm air-dry soil were finely ground (Retsch mixer mill MM200; Verder Scientific, Newtown, PA, USA) and scanned undiluted in a Bruker Vertex 70 FT-IR Spectrometer with HTS-XT (Bruker Optik GmbH, Germany). Carbonate concentration was predicted using a model calibrated with the USDA NRCS spectral library, consisting of 1238 samples collected across the USA. The entire available spectral range of 4000 - 600 cm^{-1} was used and spectra were preprocessed with multiplicative scatter correction, followed by first

derivative transformation. Carbonate was converted to IC using the molar mass of $CaCO_3$, the dominant carbonate species at the site. Soil OC concentration was determined by difference between MIR-predicted IC concentration and total C concentration for carbonate-containing samples.

2.2.4. Baseline SOC stock calculation

Soil OC stock (kg OC m^{-2}) for each depth increment was calculated as the product of oven-dry soil mass (<2-mm) and OC concentration. Cumulative soil OC stocks were converted from depth coordinates to mass coordinates using a monotonic cubic spline function with Hyman filtering (R Core Team, 2016), and further statistical analyses were performed on the cumulative soil mass layers 0-300 kg m^{-2}, 300-650 kg m^{-2}, and 0-650 kg m^{-2} (Wendt and Hauser, 2013). The upper limit of 650 kg m^{-2} was set to the minimum cumulative soil mass measured across both fields in order to avoid extrapolation with the spline function and to facilitate accurate comparisons (Goidts et al., 2009).

2.2.5. Stratification approaches

Stratification schemes were developed for both fields using soil survey data, terrain indices, and SOM_v data (Figure 2.3).

2.2.5.1. Soil survey data

Soil data were acquired from the USDA NRCS Soil Survey Geographic database for Kossuth Co, IA, USA. Soil series mapping units were used as sampling strata for the soil survey data (Figure 2.3*a*, 2.3*d*).

2.2.5.2. Terrain indices

Elevation data (Figure 2.2*a*) were acquired from a 3-m resolution DEM aggregated from 1-m resolution LiDAR data (University of Iowa Department of Natural Resources Geological and

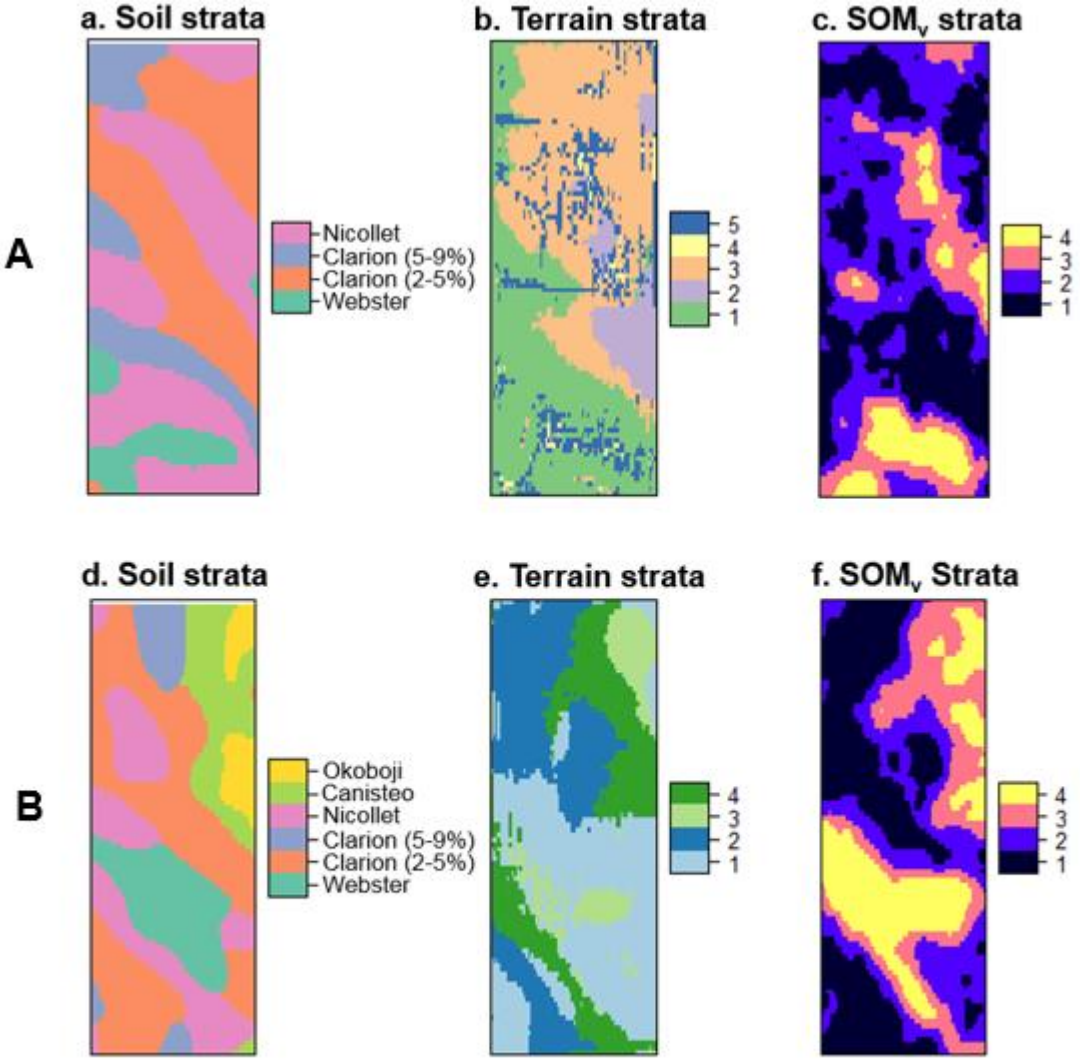

Figure 2.3 Stratification maps generated from soil survey data (**a, d**), terrain indices (**b, e**), and SOMv (**c, f**). Top panels (**a-c**) are from Field A; bottom panels (**d-f**) are from Field B. Numbers in parentheses for soil strata key are slopes.

Water Survey, 2008). Following the recommendation of Buchanan et al. (2014), slope (Figure 2.2*b*) was computed using the maximum triangular slope method of Tarboton (1997), catchment area (α) was computed using the multiple triangular flow direction algorithm of Seibert and McGlynn (2007), and the soil topographic wetness index (STI, Figure 2.2*c*) was calculated as:

$$STI = ln\left(\frac{\alpha}{Ttan(slope)}\right) \quad [1]$$

Where T is the soil transmissivity ($m^2\ d^{-1}$), which was set to the estimated representative saturated hydraulic conductivity for each soil map unit in the SSURGO database, as these soils have no restrictive layers. Flow length, flow accumulation, and both planar and horizontal curvature were also computed (Figure. 2.2*c*, 2.2*g*), as these indices have been shown to correlate with soil OC stock in other studies (Behrens et al., 2010; Lacoste et al., 2014; Wiesmeier et al., 2014; Aitkenhead and Coull, 2016). All terrain indices were calculated from DEM data using the SAGA plugin (Conrad, et al., 2015) for QGIS (ver. 2.16.3).

A principal component analysis was performed to eliminate collinearity among terrain indices and to reduce the dimensionality of the data. The values of the first three components were extracted from the raster grid cells at the coring locations, and the k-means clustering algorithm was implemented to transform the continuous terrain data from each coring location into categorical strata while minimizing within-strata variance. The percent of variance explained in the terrain data was plotted against the number of strata for a set of 1 to 12 strata, and the optimal number of strata for each field (Figure 2.3*b*, 2.3*e*) was determined by visually assessing the point at which the curve flattened out (Viscarra-Rossel, et al. 2016).

2.2.5.3. SOM_v data

Empirical semivariograms for the SOM_v data were computed and fit with a spherical model using the gstat package in R (Pebesma, 2004). SOM_v values were predicted for each soil coring location (excluding offsets) using ordinary kriging, and k-means clustering was used to transform the continuous SOM_v data from each coring location into categorical strata using the same criteria as the terrain data (Figure 2.3*c*, 2.3*f*).

2.2.6. Simulated sampling

A Monte Carlo approach was used to assess how well a reduced sample number of n=6, 12, 24, and 48 cores could reproduce the baseline mean soil OC stock for topsoil (0-300 kg soil m^{-2}), subsoil (300-650 kg soil m^{-2}), and profile (0-650 kg soil m^{-2}) soil OC stocks, estimated from 100 and 99 cores at Field A and Field B, respectively. Simple random sampling was simulated by randomly selecting grid points, calculating the mean soil OC stock, and repeating the process 1000 times. For stratified sampling using soil, SOM_v, and terrain data, the number of samples randomly selected per stratum for each simulation was weighted by the proportional area of the stratum, and mean field soil OC stock was calculated using the same weights. In order to improve spatial balance only the regular grid points were used in the Monte Carlo simulation, i.e. offset grid points were excluded. The uncertainty of each sampling approach was quantified by the RMSE.

2.2.7. Soil OC stock modeling

The stratification approach with the best performance was used to select a calibration data set for model development. Coring locations were selected from the pool of regular grid points at each site using the mean attribute value for each strata as the selection criterion. For example, for n=12, if the output of the k-means algorithm for the SOM_v data yielded four clusters, the three sampling points with SOM_v values closest to the mean would be selected from each cluster. For the terrain indices, the mean values of the first principal component was used. The remaining data points, including offsets, were designated as a validation set.

In order to remove collinearity between potential predictors, a second principle component analysis was performed on all of the available continuous variables with complete coverage of the study area: SOM_v, CEC_p, elevation, slope, STI, planar and horizontal curvature, flow accumulation, and flow length. The number of potential variables (9) was large relative to

the number of calibration data points for the lower sample numbers, so two model selection algorithms were implemented to identify the best performing model and minimize overfitting: best subsets, and the least absolute shrinkage and selection operator (LASSO). The best-subsets and LASSO-selected models were compared with a random forest model and a single variable ordinary least squares model using SOM_v as the sole predictor.

2.2.7.1. Model building

The best-subsets algorithm uses exhaustive search to identify the best subsets of the predictor variables for predicting the target variable using linear regression (Lumley, 2017). Model fitting criteria for the best subsets procedure included AIC, BIC, and Mallow's cp. The fitting criterion that included the fewest parameters in the best-fit model was chosen to minimize overfitting. The LASSO algorithm was developed to optimize the trade-off between bias and variance of a general linear model by using a tuning parameter (λ) to shrink the values of the model coefficients (Friedman, et al., 2010). K-fold cross-validation was used to identify the best solutions for λ and the coefficient values of the fitted model using the package glmnet in R (Friedman, et al., 2010).

The random forest model uses a boot-strapping approach to build a set number of classification and regression trees from a training dataset, and the predictions made with each tree are then averaged (Breiman, 2001). The R package randomForest (Liaw and Weiner, 2002) was used to build the random forest model using available predictor variables; the number of trees was set to 1000, and all predictors were compared at each node when splitting trees.

2.2.7.3. Model validation and ordinary kriging

Soil OC stocks for topsoil, subsoil, and the whole profile were predicted at the validation points with each modeling approach: best-subsets, LASSO-selected, random forest, and the

single predictor SOM_v model. Model performance was evaluated on the basis of adjusted R^2, RMSE, and the slope and intercept values for the validation regression. The best-performing model was selected, and the predicted soil OC stock for each grid point was used to generate a variogram model of spatial covariance. The variogram model was used to perform ordinary kriging, and the prediction performance of the ordinary kriging model was assessed by leave one out cross validation at each coring location. If the variogram model for predicted SOC stocks did not show spatial dependence, the SOM_v variogram model was used instead.

2.3. RESULTS

2.3.1. Baseline soil OC stocks

All soil OC stock distributions were positively skewed (Figure 2.4), and maps of soil OC stocks generated from the full dataset (n=100) revealed the presence of "hotspots", showing clearly the uneven spatial distribution of topsoil, subsoil and profile soil OC stocks at these sites (Figure 2.6). Topsoil stored a greater quantity of soil OC than subsoil for the 0-650 kg soil m^{-2} profile at both sites (Figure 2.4). Topsoil OC stock at Field A was 7.61 kg m^{-2} compared to 4.90 kg m^{-2} OC stock in the subsoil, while topsoil OC stock at Field B was 7.85 kg m^{-2} and subsoil OC stock was 4.34 kg m^{-2} (Figure 2.4). Mean soil OC stocks were not significantly different ($p > 0.05$) between Field A and Field B for topsoil, subsoil or the full profile. However, topsoil and profile soil OC stocks were more variable at Field B and the range was greater than at Field A, while subsoil OC stocks were more equally distributed between fields (Figure 2.4). Additionally, the correlation between topsoil, and both subsoil and profile OC stocks was stronger at Field B (0.64 and 0.93, respectively) than at Field A (0.44 and 0.79, respectively) (Table 2.2).

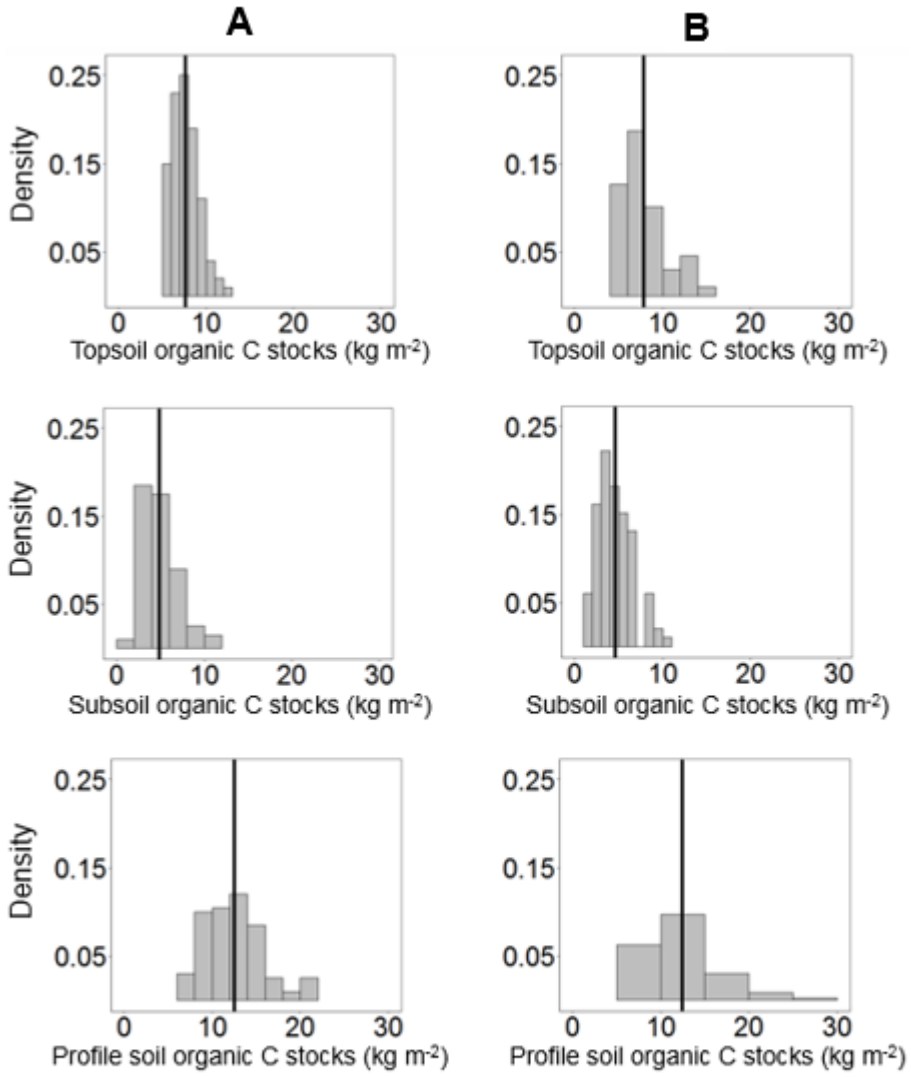

Figure 2.4 Distribution of topsoil (0-300 kg soil m^{-2}, top panels), subsoil (300-650 kg soil m^{-2}, middle panels) and profile (0-650 kg m^{-2}, bottom panels) soil organic C stocks at Field A (left column) and Field B (right column). *Bold lines indicate means.*

2.3.2. Stratification

Stratification with SOM_v was the best approach for the topsoil layer for both Field A and Field B, with the lowest RMSEs for all sample numbers (n=6, 12, 24, and 48) (Table 2.1). The distribution of predicted mean topsoil SOC stocks generated with the SOM_v stratification

approach had a much narrower interquartile range, and narrower 95% confidence intervals as well (Figure 2.5).

Table 2.1 Stratification results: root mean square error (RMSE) of mean soil organic carbon stock estimates from simulated resampling at a reduced number of samples.

		Topsoil (0-300 kg soil m^{-2})				Subsoil (300-650 kg soil m^{-2})				Profile (0-650 kg soil m^{-2})			
Field	***n***	**Random**	**Soil**	**Terrain**	**SOM_v**	**Random**	**Soil**	**Terrain**	**SOM_v**	**Random**	**Soil**	**Terrain**	**SOM_v**
		RMSE				RMSE				RMSE			
A	**6**	0.71	0.62	0.58	0.45	0.86	0.94	0.81	0.86	1.38	1.28	1.09	1.20
	12	0.52	0.43	0.46	0.32	0.64	0.65	0.61	0.65	0.95	0.96	0.88	0.86
	24	0.39	0.35	0.33	0.27	0.50	0.49	0.48	0.50	0.79	0.71	0.70	0.70
	48	0.39	0.33	0.34	0.24	0.46	0.45	0.43	0.47	0.70	0.69	0.63	0.63
B	**6**	1.05	0.92	0.89	0.80	0.93	0.97	0.94	0.95	1.81	1.72	1.66	1.60
	12	0.80	0.64	0.65	0.53	0.67	0.61	0.66	0.63	1.34	1.33	1.24	1.12
	24	0.62	0.49	0.53	0.40	0.51	0.50	0.49	0.50	1.03	0.87	0.91	0.85
	48	0.60	0.47	0.48	0.39	0.48	0.46	0.48	0.47	0.99	0.83	0.89	0.77

Random = simple random sampling, Soil = stratification by soil series map units, Terrain = stratification by terrain indices, SOM_v = stratification by on-the-go visual/near-infrared predicted soil organic matter

Terrain-based and soil survey-based stratification approaches were substantially less variable than simple random sampling for topsoil at both fields, but more variable than SOM_v stratification (Table 2.1, Figure 2.5). For the soil survey data, the strata show similar patterns to that of the SOM_v data, and have the same number of strata, but the soil strata show much coarser resolution (Figure 2.3). Both the terrain and SOM_v strata show finer spatial resolution than the soil strata, and the terrain strata have much sharper spatial boundaries than the SOM_v strata as well (Figure 2.3).

Estimates of subsoil OC stocks at Field A were slightly less variable with terrain-based stratification than with simple random sampling, soil survey, or SOM_v based stratification at all sampling intensities, while at Field B, estimates of subsoil OC stocks were equally variable for all sampling approaches (Table 2.1, Figure 2.5). Estimates of profile soil OC stocks were

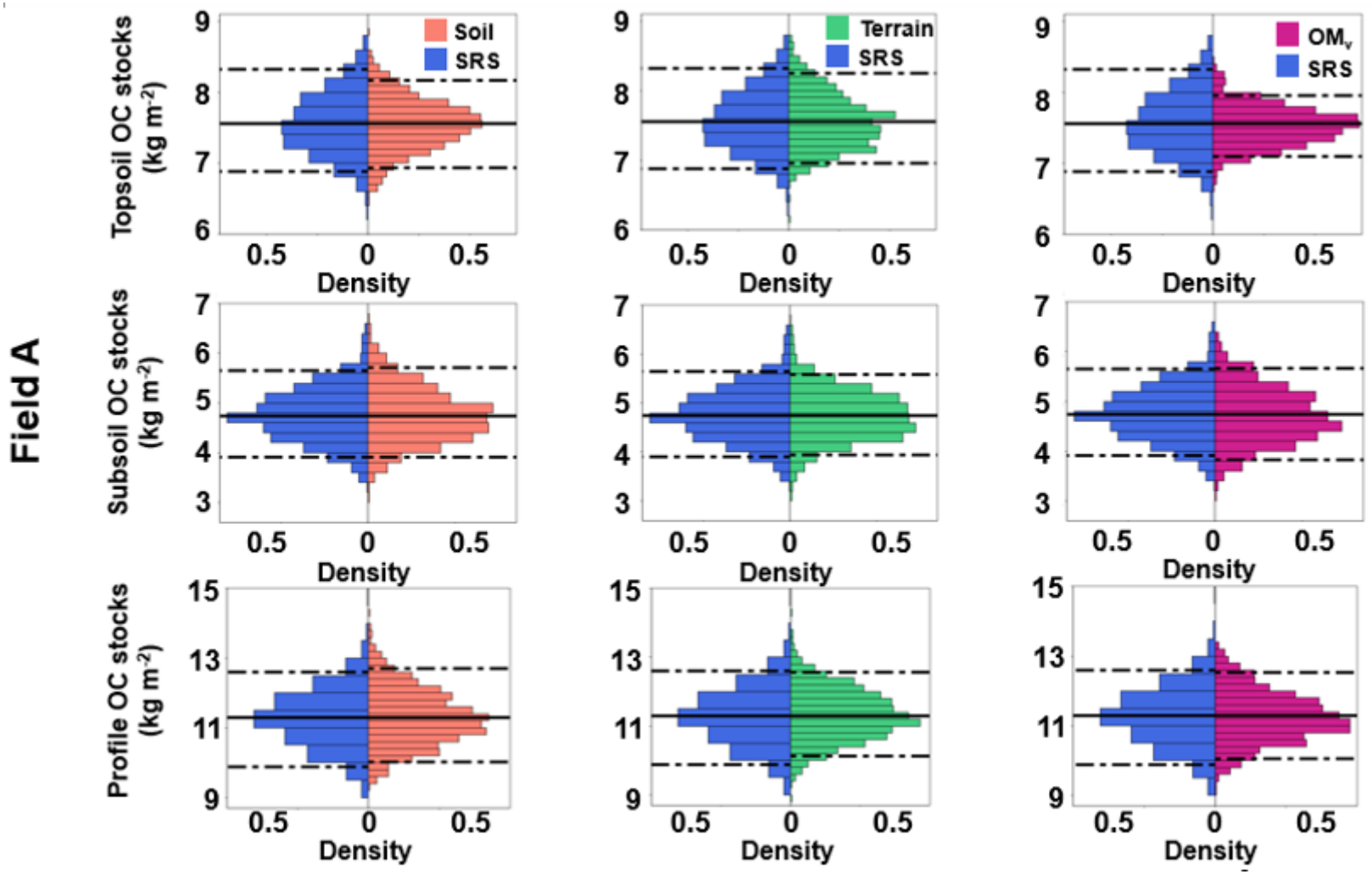

Figure 2.5 Stratification results for Field A: estimated mean SOC stocks for the topsoil (0-300 kg soil m^{-2}, **top panels**), subsoil (300-650 kg soil m^{-2}, **middle panels**), and full profile (0-650 kg soil m^{-2}, **bottom panels**) from a Monte Carlo simulation with 1000 replications and n=12 cores. Colors indicate stratification approach: blue = simple random sampling, orange = soil survey data, green = terrain indices, and purple = SOM_v. *Results for Field B were similar and are not shown.*

improved by all three stratification approaches when compared to simple random sampling at both sites for the lowest sample number (n=6), but improvements at Field B were better than at Field A for the higher sample numbers (n=12, 24, 48) (Table 2.1). Among the stratified sampling approaches, estimates of profile soil OC stocks were relatively equivalent for both sites. Stratification improved profile soil OC stock estimates more than subsoil OC stocks estimates, but not as much as estimates for topsoil (Table 2.1).

Table 2.2 Pearson's correlation coefficients for topsoil, subsoil, and full profile soil organic C stocks, and predictors.

A				B			
	Topsoil	**Subsoil**	**Profile**		**Topsoil**	**Subsoil**	**Profile**
Topsoil	1.00			Topsoil	1.00		
Subsoil	0.44	1.00		Subsoil	0.64	1.00	
Profile	0.79	0.90	1.00	Profile	0.93	0.88	1.00
STI	0.47	0.21	0.37	STI	0.62	0.38	0.56
VCUR				VCUR	-0.21		
HCUR		-0.19	-0.20	HCUR			
FLL				FLL	-0.37		-0.27
FLAC	0.27			FLAC			
ELEV	-0.24	-0.32	-0.34	ELEV	-0.58	-0.22	-0.46
Slope	-0.44		-0.13	Slope	-0.61	-0.38	-0.56
SOM_v	0.70		0.34	SOM_v	0.84	0.37	0.70
CEC	0.44		0.20	CEC	0.64		0.44

All correlations shown are significant at $p < 0.05$. STI = soil topographic wetness index; VCUR = profile curvature; HCUR = planar curvature; FLL = flow length; FLAC = flow accumulation; ELEV = elevation.

2.3.3. SOC stock modeling

Calibration data for the soil OC stock prediction models were selected from the SOM_v data for the topsoil and the full profile at both sites, as well as the subsoil at Field B, while the terrain-based stratification approach was only used to select calibration data for subsoil OC stocks at Field A, where that approach marginally outperformed SOM_v stratification (Table 2.1). Topsoil SOC stocks were predicted more accurately and with greater precision than subsoil or

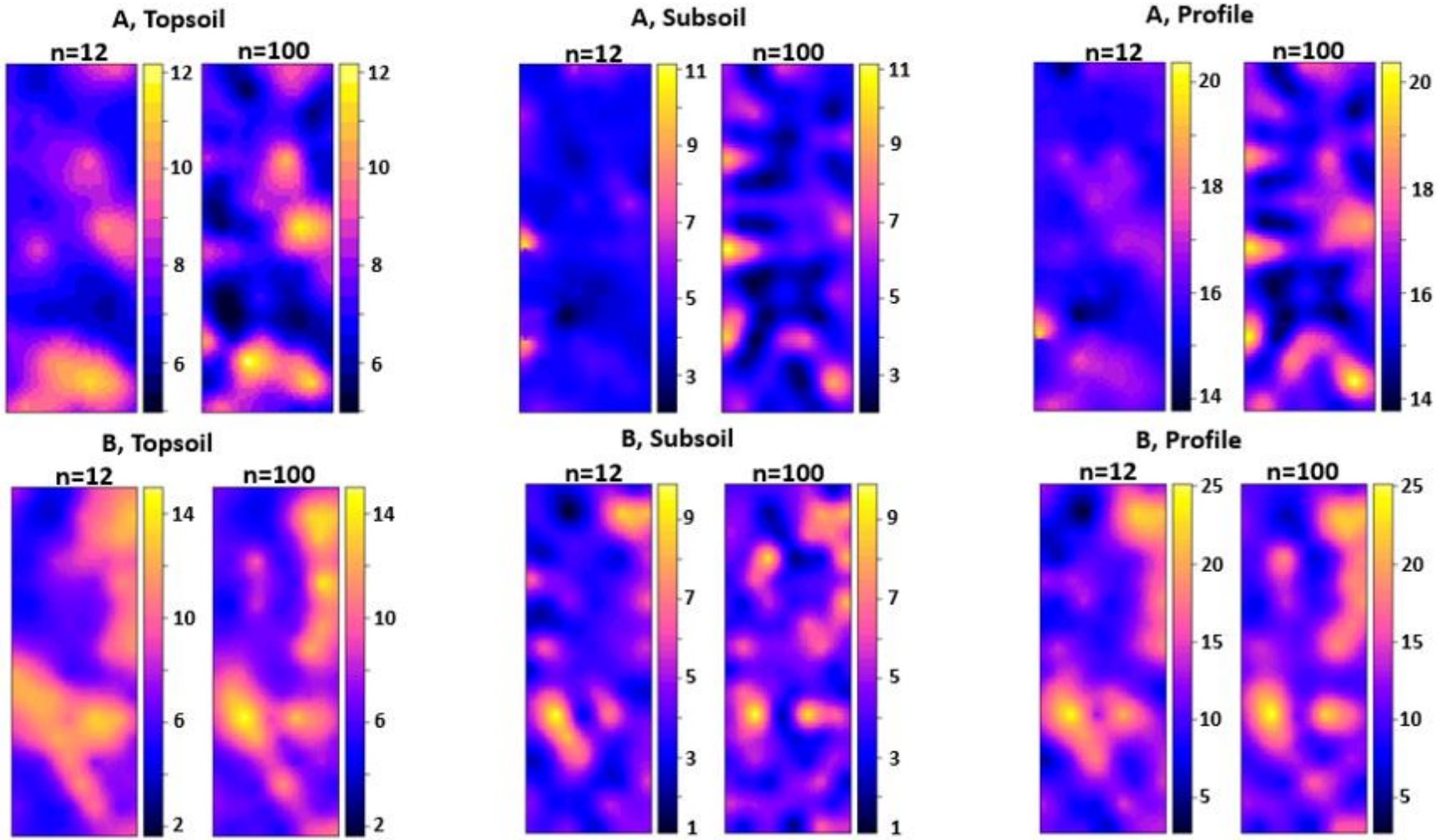

Figure 2.6 Soil organic C stock prediction maps produced from a reduced sample calibration data set (n=12) compared to predictions from the full dataset (n=100). Units are kg soil organic C m^{-2}.

profile SOC stocks at both sites (Table 2.3). Profile SOC stock predictions were only slightly less accurate than topsoil (R^2=0.53 and 0.56, for Field A and Field B, respectively), while subsoil OC stocks were predicted poorly (R^2=0.33 and 0.32, for Field A and Field B, respectively). Prediction performance was higher for Field B than Field A for both topsoil and the full profile, but similar for subsoil (Table 2.3).

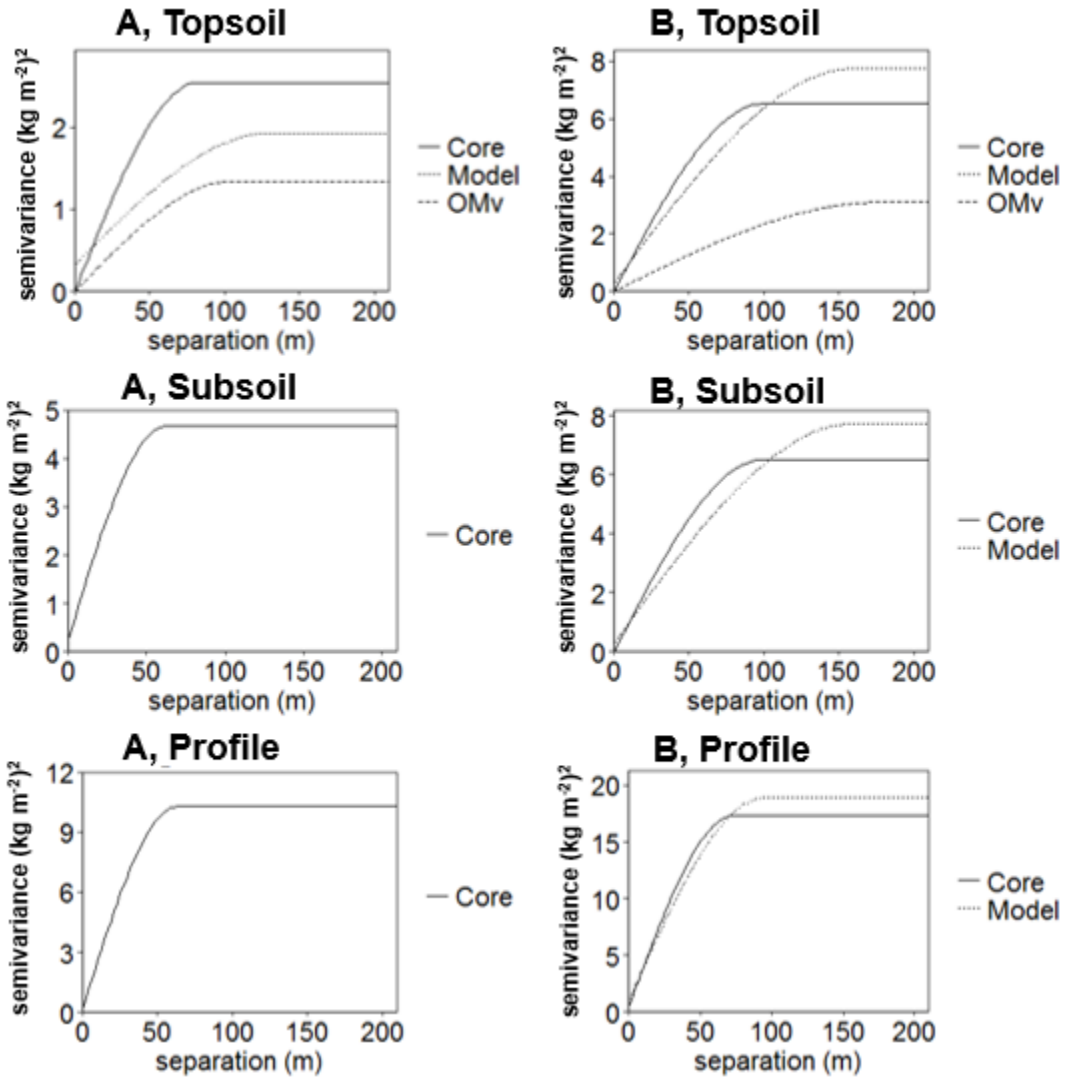

Figure 2.7 Empirical semivariograms showing the covariance in soil organic C stock with distance for soil organic C stock estimates made with measured soil core data (solid lines), model predictions (dotted lines), and SOM_v data (dashed lines). There was no spatial dependence in the model predictions of subsoil or profile OC stock at Field A, and therefore no variogram model could be developed.

The model using SOM_v as the sole predictor out-performed the more complex models in predicting topsoil SOC stocks at both Field A and Field B, with RMSEs of 1.09 and 1.44, and R^2s of 0.54 and 0.68, respectively (Table 2.3). Subsoil and profile models benefited from the inclusion of additional predictors, with the random forest models producing the best fits at Field A, and the best-subset models producing the best fits at Field B (Table 2.3). Subsoil and profile SOC stocks were predicted with low accuracy at both sites. Model prediction bias varied among models for topsoil versus subsoil and profile SOC stocks: topsoil models were positively biased, in concordance with the distribution of the full dataset (Figure 2.4), but the subsoil and profile models were all negatively biased (Table 2.3).

The range of spatial covariance in subsoil and profile OC stocks was smaller than in topsoil for both the core data, SOM_v data, and model predictions (Figure 2.6, Figure 2.7). Spherical variogram models fitted to model-predicted SOC stocks overestimated the range of spatial covariance at both sites in comparison to the core data, while the partial sill for topsoil was overestimated by the SOM_v model at Field B, but underestimated at Field A (Figure 2.7). The variogram model for predicted SOC stock showed no spatial dependence for either the subsoil or profile model at Field A (Figure 2.7). However, utilizing the variogram model developed from the SOM_v data did still improve RMSEs over the non-spatial model predictions for subsoil and profile OC stocks at Field A (Table 2.3 Figure 2.6). In all cases, adding a model of spatial covariance reduced the absolute bias of model predictions and, with the exception of profile soil OC stocks at Field B, precision was improved as well (Table 2.3).

Table 2.3 Validation statistics for the best-fit soil organic C stock prediction models at a reduced sample number (n=12) for topsoil (0-300 kg soil m^{-2}), subsoil (300-650 kg soil m^{-2}), and the full profile (0-650 kg soil m^{-2}).

Soil Mass	Field	Calibration	Model	Adjusted R^2	RMSE	Bias
kg soil m^{-2}						
0-300	A	Core	vgm	-	1.56	0.13
		SOM_v	SOM_v	0.68	1.44	0.25
		SOM_v	SOM_v + vgm*	0.68	1.31	0.10
	B	Core	vgm	-	1.10	-0.07
		SOM_v	SOM_v	0.54	1.09	0.19
		SOM_v	SOM_v + vgm	0.54	0.97	-0.01
300-650	A	Core	vgm	-	1.88	0.01
		SOM_v	PC1 + PC5 + PC6 + PC9	0.32	1.78	-0.41
		SOM_v	PC1 + PC5 + PC6 + PC9 + vgm	0.32	1.53	0.07
	B	Core	vgm	-	1.60	0.15
		SOM_v	Random forest (PC1:PC9)	0.33	2.20	-0.57
		Terrain	Random forest (PC1:PC9) + vgm*	0.33	1.34	-0.04
0-650	A	Core	vgm	-	3.12	0.11
		SOM_v	PC1 + PC2 + PC5 + PC6 + PC7 + PC9	0.56	3.03	-0.48
		SOM_v	PC1 + PC2 + PC5 + PC6 + PC7 + PC9 + vgm	0.56	3.16	0.19
	B	Core	vgm	-	2.40	-0.21
		SOM_v	Random forest (PC1:PC9)	0.53	3.67	-0.89
		SOM_v	Random forest (PC1:PC9) + vgm*	0.53	1.66	-0.03

Uncertainty estimates for core data are the output of the leave-one-out cross validation exercise for the ordinary kriging model. Fit statistics are presented for the non-spatial models as well as combined with an ordinary kriging model (+ vgm). For model predictions with no spatial structure, the SOM_v variogram model was used (vgm*). RMSE = root mean square error.

2.4. DISCUSSION

2.4.1 Stratification

Soil OC stocks followed an approximately log-normal distribution for topsoil, subsoil, and the full profile at both of the sites assessed in this study. The skewed distribution was due to "hotspots" of soil OC stock occurring in localized areas within the field. According, simple random sampling was not an efficient method for assessing baseline soil OC stocks, requiring a higher number of samples to reach the same level of precision for estimating mean topsoil and profile soil OC stocks compared with stratified sampling.

The relatively poor performance of soil survey data for stratification indicates that soil series map units were inadequate for representing the variation in either topsoil or subsoil SOC stocks at these 11 ha field sites. The lack of explanatory power of soil series for predicting SOC stocks has been noted by other authors as well (Minasny, et al., 2013), and is likely due to the coarse scale at which the soils are mapped, as the variation of SOC stocks is relatively high within soil series map units. Additionally, delineations may be made between soils that have similar soil OC content, but differ in other soil properties. For example, the mean soil OC stock content of the Webster soil is not significantly different ($p > 0.05$) than that of the Okoboji soil at Field B, nor are soil OC stocks significantly different ($p > 0.05$) between the Clarion soil with 2-5% slopes and the Clarion soil with 5-9% slopes at Field A.

Compared to simple random sampling, stratification with terrain indices improved baseline soil OC stock estimates for topsoil and the full profile, although improvements in subsoil OC stock estimates were marginal. These results suggest that these data are more relevant than soil survey data for field-scale SOC stock assessment, particularly as they are available a much finer spatial resolution. Terrain indices improved stratification performance more at Field B than at Field A, and this is likely due to the stronger correlations between soil OC stocks and slope, elevation, and STI at Field B. This pattern of correlation, in conjunction with the stronger correlation between topsoil and subsoil OC stocks, may be due to higher rates of erosion at Field B increasing the redistribution of soil OC from sloped, higher elevation areas to low-lying areas. The explanation for this may be that the soil on Field A is less susceptible to erosion due to the inclusion of a winter cover crop (*Avena sativa*) and the biennially grown *Medicago sativa* in the cropping rotation, compared to Field B which is fallow in the winter. This

conclusion is also supported by the observation that topsoil OC stocks were significantly lower for the Clarion soils mapped with 5-9% slopes than 2-5% slopes at Field B, but not at Field A. The results of the simulated resampling suggest that the stratification schemes tested in this study are effective for topsoil and 0-650 kg soil m^{-2} soil profiles, but only marginally useful for subsoil. The lack of substantial improvement in subsoil OC stock estimates with any of the stratification approaches is likely in part due to the relatively weak relationship between the stratification variables and subsoil OC stocks in this study (Table 2.2). However, the distribution of mean subsoil OC stock estimates from the SOM_v and terrain stratification approaches more closely matched the true distribution of subsoil OC stocks than did the simple random sampling approach, accurately capturing the positive skew. This may indicate that the greater variability in subsoil OC stocks cannot be adequately represented at the same sampling density as topsoil OC stocks for these sites.

Another factor may also be the difference in resolution of the sampling grid in comparison to the stratification data. The sampling grid spacing of 42m was chosen to provide spatially balanced coverage of the study area with the 100 soil core samples we could afford to collect. However, the range of spatial covariance in subsoil OC stock is smaller than in topsoil (Figure 2.7), and therefore the sampling grid resolution used may be too coarse to capture the nuances of the covariance of subsoil OC stocks with the stratification variables.

2.4.2. Soil OC stock modeling

Topsoil OC stock predictions using SOM_v-optimized sampling with a sampling intensity of just over 1 soil core per ha (n=12) and SOM_v as the sole predictor had both good prediction accuracy and high precision, outperforming more complex models that utilized additional information such as soil series or terrain indices. Although generating SOM_v data is a

complicated process, since these data can be provided for a low cost as a commercial service, using a single predictor SOM_v model is less complex from a modeling perspective than building a model with many predictors generated from a principal component analysis. The high performance of the SOM_v data indicates that these spectroscopic measurements made in the top 0.05 m can adequately capture the variation in soil OC stocks to a depth of 0.30 m at these sites, and suggests that the processes controlling SOC stock in the top 0.05 m are similar to those that dominate to a depth of 0.30 m.

The relatively high performance of profile soil OC stock predictions, compared to subsoil, is due to the dominance of topsoil OC stocks for the 0-650 kg m^{-2} (0-0.75 m) soil profiles measured (Table 2.3). The best models for predicting profile soil OC stocks utilized terrain indices in addition to the proximal sensing data (SOM_v and CEC), indicating that the terrain indices measured in this study are relevant for explaining soil OC dynamics below common sampling depths of 0.2 or 0.3 m. The best prediction models for subsoil also utilized terrain indices in addition to proximal sensing data, however, subsoil models were still relatively inaccurate, indicating that the variables measured in this study were not adequate for fully explaining the observed variation in subsoil OC stocks.

The lack of improvement in subsoil OC stock models compared to the gain in model performance for profile soil OC stocks when terrain indices were included may also be an artifact of the distinction between topsoil and subsoil. Definitions of topsoil and subsoil in this study were based on a review of the soil C assessment literature, which focuses largely on the 0-0.2 m or 0-0.3 m depth layer. In reality, the soil profile is continuous, and while the topsoil may be recognizable as distinct from the subsoil, particularly in tilled arable soils, the boundaries of these soil layers varies in 3-dimensions. Accordingly, designing future soil OC assessment

schemes in a way that incorporates this flexibility may improve our understanding of topsoil versus subsoil OC dynamics.

The results of this study show that VNIR-p can be used to capture the full range of topsoil SOC stock variance at the field scale, including "hotspots", and can be used to develop an empirical variogram for mapping topsoil SOC stocks. SOM_v data was particularly useful for improving model predictions of subsoil SOC stock when topsoil and subsoil OC stocks were well correlated, for example at Field B in this study, but was an insignificant significant predictor of subsoil OC stocks at Field A. However the importance of topsoil OC stocks for mapping and modeling profile soil OC stocks suggests that commercially provided SOM_v data is a promising data source for full profile soil OC stock assessment, not just for topsoil. This finding is supported by both the stratification and modeling results presented in this study.

The improvements in model precision gained from incorporating a model of spatial covariance show that calibrating high resolution remote and proximal sensing data with a minimal number of direct observations is an effective approach for low-cost mapping of soil OC stocks, but that future studies should assess other soil properties that can be measured with these technologies that may be better predictors of subsoil OC stocks.

2.5. CONCLUSIONS

Based on the results of this study, we recommend that SOC assessment should be designed for subsoil as well as topsoil SOC stock, and for spatial modeling a grid spacing closer than 42 m may be necessary to capture the shorter range of variation observed in the distribution of subsoil OC stocks. We recommend that subsoil and topsoil SOC stocks should either be modeled separately or, preferably, using a continuous function that allows for distinct dynamics

in the upper and lower soil profile. The non-normal distribution suggests that using a simple mean for soil OC stock assessment at the field scale could be misleading if soil OC stock "hotspots" arise from differential rates of soil OC cycling, and underscores the importance of mapping to fully capture the variance in soil OC stocks at the field scale. Lacking the knowledge of how soil carbon is distributed in space prevents us from understanding how carbon stocks change in response to environmental conditions over time, thus understanding this spatial distribution is essential to the development of best-management practices that will increase soil C sequestration. Spatially explicit soil OC stock assessment allows for the targeting of specific sampling locations in the future, potentially improving monitoring as well as baseline estimates of soil OC stocks.

2.6. REFERENCES

Aitkenhead, M.J., and M.C. Coull. 2016. Mapping soil carbon stocks across Scotland using a neural network model. Geoderma 262: 187–198 Available at http://linkinghub.elsevier.com/retrieve/pii/S0016706115300628.

Allen, D.E., M.J. Pringle, K.L. Page, and R.C. Dalal. 2010. A review of sampling designs for the measurement of soil organic carbon in Australian grazing lands. Rangel. J. 32(2): 227–246.

Batjes, N.H., I.S. Reference, I.C. Isric, P.O. Box, and A.J. Wageningen. 1996. Total carbon. Eur. J. Soil Sci. 47(June): 151–163.

Behrens, T., K. Schmidt, a. X. Zhu, and T. Scholten. 2010. The ConMap approach for terrain-based digital soil mapping. Eur. J. Soil Sci. 61(1): 133–143.

Breiman, L. 2001. Random Forests, Machine Learning 45(1): 5-32.

Bricklemyer, R.S., and D.J. Brown. 2010. On-the-go VisNIR: Potential and limitations for mapping soil clay and organic carbon. Comput. Electron. Agric. 70(1): 209–216.

Buchanan, B., M. Fleming, R. Schneider, B. Richards, J. Archibald, Z. Qiu, M. Walter. 2014. Evaluating topographic wetness indices across central New York agricultural landscapes. Hydrol. and Earth Syst. Sci. 18(8): 3279-3299.

Chabbi, A., J. Lehmann, P. Chabbi, H.W. Loescher, M.F. Cotrufo, A. Don, M. SanClements, L. Schipper, J. Six, P. Smith, and C. Rumpel. 2017. Aligning agriculture and climate policy. Nat. Clim. Chang. 7(5): 307–309 Available at http://www.nature.com/doifinder/10.1038/nclimate3286.

Ciais, P., C. Sabine, G. Bala, L. Bopp, V. Brovkin, J. Canadell, A. Chhabra, R. DeFries, J. Galloway, M. Heimann, C. Jones, C. Le Quéré, R.B. Myneni, S. Piao, and P. Thornton. 2013. Carbon and Other Biogeochemical Cycles. Clim. Chang. 2013 - Phys. Sci. Basis: 465–570 Available at http://www.ipcc.ch/report/ar5/wg1/docs/review/WG1AR5_SOD_Ch06_All_Final.pdf%5Cnhttp://ebooks.cambridge.org/ref/id/CBO9781107415324A023%0A

Conrad, O., Bechtel, B., Bock, M., Dietrich, H., Fischer, E., Gerlitz, L., Wehberg, J., Wichmann, V., and Böhner, J. (2015): System for Automated Geoscientific Analyses (SAGA) v. 2.1.4, Geosci. Model Dev., 8, 1991-2007, doi:10.5194/gmd-8-1991-2015.

de Gruijter, J.J., D.J. Brus, M.F.P. Bierkens, and M. Knotters. 2006. Sampling for Natural Resource Monitoring. Springer.

de Gruijter, J.J., A.B. McBratney, B. Minasny, I. Wheeler, B.P. Malone, and U. Stockmann. 2016. Farm-scale soil carbon auditing. Geoderma 265: 120–130 Available at http://dx.doi.org/10.1016/j.geoderma.2015.11.010.

Friedman, J., Hastie, T. and Tibshirani, R. (2010) Regularization paths for generalized linear models via coordinate descent. J. Statist. Sofwr., 33, no.1.

Gebbers, R.; Lück, E.; Dabas, M.; Domsch, H. 2009. Comparison of instruments for geoelectrical soil mapping at the field scale. Near Surface Geophysic 7: 179-190.

Gebbers, R, and V. Adamchuk. 2010. Science. 327:828-31. doi: 10.1126/science.1183899.

Goidts, E., V. van Wesemael, and M. Crucifix. 2009. Magnitude and sources of uncertainties in soil organic carbon (SOC) stock assessments at various scales. Eur. J. Soil Sci. 60(5): 723-739.

Hobley, E., B. Wilson, A. Wilkie, J. Gray, and T. Koen. 2015. Drivers of soil organic carbon storage and vertical distribution in Eastern Australia. Plant Soil 390(1–2): 111–127 Available at http://link.springer.com/10.1007/s11104-015-2380-1.

Jague, E.A., M. Sommer, N.P.A. Saby, J. Cornelis, B. Van Wesemael, and K. Van Oost. 2016. Soil & Tillage Research High resolution characterization of the soil organic carbon depth profile in a soil landscape affected by erosion. Soil Tillage Res. 156: 185–193 Available at http://dx.doi.org/10.1016/j.still.2015.05.014.

Jobbágy, E.G., and R.B. Jackson. 2000. The Vertical Distribution of Soil organic carbon and its ecological applications. 10(2): 423–436 Available at http://www.esajournals.org/doi/abs/10.1890/1051-0761(2000)010%5B0423:TVDOSO%5D2.0.CO;2.

Knadel, M., A. Thomsen, K. Schelde, M. Greve. 2015. Soil organic carbon and particle sizes mapping using vis–NIR, EC and temperature mobile sensor platform. Computers and Electronics in Agriculture, 114: 134-144.

Koarashi, J, W. Hockaday, C. Masiello, S. Trumbore. 2012. Dynamics of decadally cycling carbon in subsurface soils. J. of Geophys. Res., 117: G03033, doi:10.1029/2012JG002034.

Koch A, McBratney A, Adams M, Field D, Hill R, Crawford J, Minasny B, Lal R, Abbott L, O'Donnell A, Angers D, Baldock J, Barbier E, Binkley D, Parton W, Wall DH, Bird M, Bouma J, Chenu C, Blora CB, Goulding K, Brunwald S, Hempel J, Jastrow J, Lehmann J, Lorenz K, Morgan CL, Rice CW, Whitehead D, Young I and Zimmerman M 2013 Soil security: solving the global soil crisis. *Global Policy* 4, 434-441.

Lacoste, M., B. Minasny, A. McBratney, D. Michot, V. Viaud, and C. Walter. 2014. High resolution 3D mapping of soil organic carbon in a heterogeneous agricultural landscape. Geoderma 213: 296–311 Available at http://dx.doi.org/10.1016/j.geoderma.2013.07.002.

Lehmann, J., and M. Kleber. 2015. Perspective The contentious nature of soil organic matter. Nature: 1–9 Available at http://dx.doi.org/10.1038/nature16069.

Liaw, A., and M. Wiener. 2002. Classification and regression by randomForest. R News 2(3), 18--22.

Liu, F., D.G. Rossiter, X.-D. Song, G.-L. Zhang, R.-M. Yang, Y.-G. Zhao, D.-C. Li, and B. Ju. 2016. A similarity-based method for three-dimensional prediction of soil organic matter concentration. Geoderma 263: 254–263. Available at http://linkinghub.elsevier.com/retrieve/pii/S0016706115001676.

Lumley, T. Leaps: regression subset selection. R package version 3.0. https://CRAN.R-project.org/package=leaps.

Mathieu, J.A., C. Hatté, J. Balesdent, and É. Parent. 2015. Deep soil carbon dynamics are driven more by soil type than by climate: a worldwide meta-analysis of radiocarbon profiles. Glob. Chang. Biol.: n/a-n/a Available at http://www.ncbi.nlm.nih.gov/pubmed/26119088.

Meersmans, J., B. van Wesemael, F. De Ridder, and M. Van Molle. 2009. Modelling the three-dimensional spatial distribution of soil organic carbon (SOC) at the regional scale (Flanders, Belgium). Geoderma 152(1–2): 43–52 Available at http://dx.doi.org/10.1016/j.geoderma.2009.05.015.

Minasny, B., B.P. Malone, A.B. McBratney, D.A. Angers, D. Arrouays, A. Chambers, V. Chaplot, Z.S. Chen, K. Cheng, B.S. Das, D.J. Field, A. Gimona, C.B. Hedley, S.Y. Hong, B. Mandal, B.P. Marchant, M. Martin, B.G. McConkey, V.L. Mulder, S. O'Rourke, A.C. Richer-de-Forges, I. Odeh, J. Padarian, K. Paustian, G. Pan, L. Poggio, I. Savin, V. Stolbovoy, U. Stockmann, Y. Sulaeman, C.C. Tsui, T.G. Vagen, B. van Wesemael, and L. Winowiecki. 2017. Soil carbon 4 per mille. Geoderma 292: 59–86 Available at http://dx.doi.org/10.1016/j.geoderma.2017.01.002.

Minasny, B., A.B. McBratney, B.P. Malone, and I. Wheeler. 2013. Digital Mapping of Soil Carbon. Elsevier.

Paustian, K., J. Lehmann, S. Ogle, D. Reay, G.P. Robertson, and P. Smith. 2016. Climate-smart soils. Nature 532(7597): 49–57 Available at http://www.nature.com/doifinder/10.1038/nature17174.

Pebesma, E.J., 2004. Multivariable geostatistics in S: the gstat package. Computers & Geosciences 30 (7), 683-691.

Rumpel, C., K. Baumann, L. Remusat, M.-F. Dignac, P. Barré, D. Deldicque, G. Glasser, I. Lieberwirth, and A. Chabbi. 2015. Nanoscale evidence of contrasted processes for root-derived organic matter stabilization by mineral interactions depending on soil depth. Soil Biol. Biochem. 85: 82–88 Available at http://www.sciencedirect.com/science/article/pii/S0038071715000620.

Rumpel, C., and I. Kögel-Knabner. 2011. Deep soil organic matter-a key but poorly understood component of terrestrial C cycle. Plant Soil 338(1): 143–158.

Salomé, C., N. Nunan, V. Pouteau, T.Z. Lerch, and C. Chenu. 2010. Carbon dynamics in topsoil and in subsoil may be controlled by different regulatory mechanisms. Glob. Chang. Biol. 16: 416–426.

Schrumpf, M., K. Kaiser, G. Guggenberger, T. Persson, I. Kögel-Knabner, and E.D. Schulze. 2013. Storage and stability of organic carbon in soils as related to depth, occlusion within aggregates, and attachment to minerals. Biogeosciences 10(3): 1675–1691.

Seibert, J. and McGlynn, B. L.: A new triangular multiple flow direction algorithm for computing upslope areas from gridded digital elevation models, Water Resour. Res., 43, W04501, doi:10.1029/2006WR005128, 2007.

Sherpa, S.R., D.W. Wolfe, and H.M. van Es. 2016. Sampling and Data Analysis Optimization for Estimating Soil Winter Coveranic Carbon Stocks in Agroecosystems. Soil Sci. Soc. Am. J. 80(5): 1377 Available at https://dl.sciencesocieties.org/publications/sssaj/abstracts/80/5/1377.

Simbahan, G.C., and A. Dobermann. 2006. Sampling optimization based on secondary information and its utilization in soil carbon mapping. Geoderma 133(3–4): 345–362.

Smith, P., C. a. Davies, S. Ogle, G. Zanchi, J. Bellarby, N. Bird, R.M. Boddey, N.P. McNamara, D. Powlson, A. Cowie, M. van Noordwijk, S.C. Davis, D.D.B. Richter, L. Kryzanowski, M.T. van Wijk, J. Stuart, A. Kirton, D. Eggar, G. Newton-Cross, T.K. Adhya, and A.K. Braimoh. 2012. Towards an integrated global framework to assess the impacts of land use and management change on soil carbon: Current capability and future vision. Glob. Chang. Biol. 18(7): 2089–2101 Available at http://doi.wiley.com/10.1111/j.1365-2486.2012.02689.x (verified 19 July 2014).

Soil Survey Laboratory Staff. 2004. Soil survey laboratory methods manual. Soil Surv. Invest. Rep. 42, Version 4.0. US Gov. Print. Office, Washington, DC.

Sudduth, K.A., N.R. Kitchen, W.J. Wiebold, W.D. Batchelor, G.A. Bollero, D.G. Bullock, D.E. Clay, H.L. Palm, F.J. Pierce, R.T. Schuler, and K.D. Thelen. 2005. Relating apparent electrical conductivity to soil properties across the north-central USA. Comput. Electron. Agric. 46(1–3 SPEC. ISS.): 263–283.

Tarboton, D. G.: A new method for the determination of flow directions and upslope areas in grid digital elevation models, Water Resour. Res., 33, 309–319, doi:10.1029/96WR03137, 1997.

Viscarra Rossel, R.A., D.J. Brus, C. Lobsey, Z. Shi, and G. McLachlan. 2016. Baseline estimates of soil organic carbon by proximal sensing: Comparing design-based, model-assisted and model-based inference. Geoderma 265: 152–163 Available at http://dx.doi.org/10.1016/j.geoderma.2015.11.016.

Wendt, J.W., and S. Hauser. 2013. An equivalent soil mass procedure for monitoring soil organic carbon in multiple soil layers. Eur. J. Soil Sci. 64(1): 58-65.

Wiesmeier, M., R. Hübner, P. Spörlein, U. Geuß, E. Hangen, A. Reischl, B. Schilling, M. von Lützow, and I. Kögel-Knabner. 2014. Carbon sequestration potential of soils in southeast Germany derived from stable soil organic carbon saturation. Glob. Chang. Biol. 20(2): 653–65 Available at http://www.ncbi.nlm.nih.gov/pubmed/24038905 (verified 22 August 2014).

Wolfe DW. 2013. Climate change solutions from the agronomy perspective. IN: Hillel D and C Rosenzweig (eds). Handbook of Climate Change and Agroecosystems: Global and Regional Aspects and Implications. Chapter 2. Imperial College Press. London.